Food Research International 246 (2026) 121157



Contents lists available at ScienceDirect

Food Research International

journal homepage: www.elsevier.com/locate/foodres





Discrimination of New Zealand wines by geographical origin and grape variety using ^{1}H NMR metabolomic fingerprinting combined with chemometric and machine learning approaches

Bruno Toribio de Lima Xavier [a], Rushan Dissanayake Mudiyanselage [a], Adrian Owens [a], Oxana Ye Rodionova [b], Alexey L. Pomerantsev [b], Daniel Granato [a,*]

[a] AUT Future Foods and Health Research Centre. Department of Biomedical, Chemical, and Food Sciences, School of Science, Faculty of Health and Environmental Sciences, Auckland University of Technology, Auckland 1010, New Zealand
[b] Federal Research Center for Chemical Physics RAS, Kosygin St. 4, 119991 Moscow, Russia

ARTICLE INFO

Keywords:
Food traceability
Wine authentication
New Zealand wines
Geographical origin
Machine learning

ABSTRACT

A total of 111 commercial New Zealand wines comprising Syrah ($n = 27$), Pinot Noir ($n = 30$), Sauvignon Blanc ($n = 28$), and Chardonnay ($n = 26$) produced in the North Island ($n = 41$) or South Island ($n = 70$) were analysed using untargeted proton nuclear magnetic resonance (^{1}H NMR) fingerprinting. Experimental results were modelled using Random Forest (RF), Support Vector Machines (SVM), Artificial Neural Networks (ANN), Automated Network Search (ANS), Data-Driven Soft Independent Modelling of Class Analogy (DD-SIMCA), Partial Least Squares – Discriminant Analysis (PLS-DA), and Soft Binary PLS-DA, aiming to authenticate wine geographical origin and varietal. Results show that varietal classification generally performed better than geographical-origin classification. SVM and RF achieved mean one-versus-rest accuracies of 97.7% and 96.0%, with mean class-specific Matthews correlation coefficients (MCCs) of 0.942 and 0.893, respectively. The best-performing ANS model correctly classified 110 of 111 wines, achieving 99.1% overall multiclass accuracy and a mean class-specific MCC of 0.988. Exploratory vintage classification achieved overall accuracies of 44.1% for SVM and 48.6% for RF; however, the uneven vintage distribution prevented these results from excluding potential vintage confounding. Hard-decision PLS-DA achieved a mean class efficiency (TEFF) of 99.4%, with one Pinot Noir sample misclassified as Syrah. For geographical-origin discrimination, SB-PLSDA achieved a TEFF of 98.2%, sensitivity of 97.2%, and specificity of 99.1% after excluding two outliers. Leave-One-Variable-Excluded-based selection improved DD-SIMCA specificity against the nearest alternative variety to 81.5–92.3%. These findings support the potential of ^{1}H NMR fingerprinting for New Zealand wine discrimination and authentication.

1. Introduction

Wine production and trade are economically important, high-value agricultural activities. Although global wine consumption declined to 214.2 million hectolitres in 2024, the lowest level since 1961, the international wine trade remained resilient, reaching €35.9 billion in export value, largely supported by elevated average export prices (€3.6 L^{-1}) and the continuing trend of premiumisation (International Organisation of Vine and Wine Intergovernmental Organisation, 2025). In this context, geographical identity and the grape varieties used to produce different types of wine have gained economic significance within this expanding market. New Zealand is internationally recognised as a prominent wine-producing country and has established a global reputation for its commitment to environmental sustainability (New Zealand Wine, 2025). Among the grape varieties cultivated in New Zealand, Sauvignon Blanc has become the country's flagship wine style, helping establish New Zealand's international wine reputation and driving wine exports (New Zealand Wine, 2025). At the same time, recognition of the quality and potential of other grape varieties, including Pinot Noir, Syrah, and Chardonnay, has grown.

New Zealand's winegrowing regions span the North and South Islands and feature diverse climates, soils, and grape-variety

* Corresponding author.
E-mail address: daniel.granato@aut.ac.nz (D. Granato).

https://doi.org/10.1016/j.foodres.2026.121157
Received 26 September 2026; Received in revised form 21 October 2026; Accepted 31 October 2026
Available online 1 November 2026
0963-9969/© 2026 The Authors. Published by Elsevier Ltd. This is an open access article under the CC BY license (http://creativecommons.org/licenses/by/4.0/).

distributions (New Zealand Winegrowers, 2026). Marlborough combines cool growing conditions with high sunshine hours and is associated with Sauvignon Blanc, while Central Otago is renowned for Pinot Noir. In the North Island, Hawke's Bay is an important region for Chardonnay and Syrah. These regional patterns do not represent a uniform climatic division between islands, as cool-climate viticulture also occurs in North Island regions such as Wairarapa. Environmental differences can influence grape development and composition, while variation also occurs within individual regions (Bramley et al., 2023; Dal Santo et al., 2016). Accordingly, the North–South Island distinction was adopted here as a broad geographical grouping for evaluating wine discrimination, while recognising the environmental and viticultural heterogeneity within each island. Beyond its environmental and oenological relevance, the wine industry represents an important component of New Zealand's economy. The sector contributes approximately NZ $2.12 billion in exports, with export volume reaching over 300 million litres (New Zealand Winegrowers, 2026).

Wines contain hundreds of metabolites derived from grape metabolism, viticultural conditions, and winemaking processes, including fermentation. These compounds influence wine quality, sensory characteristics, and varietal differentiation (Roullier-Gall et al., 2016). White wines are generally characterised by higher relative abundances of hydroxycinnamic acids and volatile thiol precursors, which contribute to citrus, tropical fruit, and herbaceous aromas, whereas red wines contain higher concentrations of anthocyanins, tannins, and flavan-3-ols, compounds responsible for wine colour, astringency, and mouthfeel (Delić et al., 2024; Han et al., 2022; Muhl et al., 2025). Environmental factors also shape wine composition. Soil properties influence vine water status, nutrient availability, and grape metabolism, affecting the accumulation of primary and secondary metabolites and contributing to terroir expression (Karapetsas et al., 2023; Priyadharshini et al., 2025). As a result, wines from different grape varieties and geographical regions may exhibit distinctive chemical fingerprints (e.g., carbohydrates, volatile organic compounds, amino acids, and phenolic compounds); however, within a grape variety, geographical effects can differ among chemical constituents and vintages (Keller et al., 2021).

Wine fingerprinting refers to characterising chemical profiles generated by numerous metabolites that reflect grape variety, geographical origin, environmental conditions, viticultural practices, and winemaking techniques. Modern metabolomics, coupled with chemometric approaches, can identify these multidimensional signatures and has become a practical tool for wine authentication, traceability, and origin discrimination (Bambina et al., 2024; Le Mao, Da Costa, & Richard, 2023). Gougeon et al. (2009) showed that wines' chemical diversity reflects geographical origin, while Tzachristas et al. (2021) highlighted the value of metabolomic and chemometric approaches for wine authentication and origin determination. New Zealand wines are recognised as speciality products because their quality and typicity are linked to geographically distinct wine-growing regions. While the Ministry for Primary Industries (2003) establishes requirements for wine identity, labelling, safety, and export eligibility, analytical authentication remains important for independently verifying provenance claims and protecting regional reputations. Consequently, analytical approaches for wine authentication are needed to independently verify provenance claims, protect consumers and producers from fraud, and evaluate the effectiveness of existing regulatory safeguards within the New Zealand wine sector.

Several analytical approaches have been proposed for wine authentication, including lipidomic profiles based on ultra-performance liquid chromatography–time–of–flight tandem mass spectrometry (UPLC-TOF-MS/MS) (Phan & Tomasino, 2021), mineral fingerprinting based on particle-induced X-ray emission (PIXE) (Bobáľ et al., 2025), inductively coupled plasma – mass spectrometry (ICP-MS) and fluorescence fingerprinting using absorbance and transmission excitation-emission matrix (A-TEEM) (Ranaweera et al., 2021), and the fusion of proton nuclear magnetic resonance (^{1}H NMR) and Raman spectroscopy (Hategan et al., 2024). However, most studies have used relatively small datasets (≤90 samples) with limited representation of New Zealand wines. A recent study of 116 New Zealand Pinot Noir wines achieved over 75% accuracy in classifying wines from three producing regions (Su et al., 2025), but its focus on a single cultivar and a limited geographical range highlights the need for broader investigations encompassing additional grape varieties and New Zealand viticultural regions.

In this context, the present study evaluated the potential of untargeted ^{1}H NMR metabolomic fingerprinting, combined with chemometric and machine-learning approaches, to discriminate and authenticate New Zealand wines by grape variety and geographical origin. Unlike previous studies, the work integrates multiple classification and authentication strategies, including Partial Least Squares – Discriminant Analysis (PLS-DA), Soft Binary PLSDA (SB-PLSDA), Data Driven - Soft Independent Modelling of Class Analogy (DD-SIMCA), Random Forest (RF), Support Vector Machines (SVM), Artificial Neural Networks (ANN), and Automated Network Search (ANS), within a single analytical framework. By comparing the performance of discrimination- and authentication-based models across 111 commercially available New Zealand red and white wines, this study provides a comprehensive assessment of untargeted ^{1}H NMR metabolomics' potential for wine traceability and provenance verification in New Zealand.

2. Materials and methods

2.1. Reagents

Potassium dihydrogen phosphate (KH_2PO_4), deuterium oxide (D_2O), 3-(trimethylsilyl)propionic-2,2,3,3-d$_4$ (TSP-d$_4$) sodium salt were purchased from Merck KGaA (Darmstadt, Germany), sodium azide (NaN_3) was purchased from BDH Limited Poole (Dorset, England), and phosphoric acid (H_3PO_4) was purchased from Sigma-Aldrich (Steinheim, Germany). D_2O was used as the lock solvent and 3-(trimethylsilyl)propionic-2,2,3,3-d$_4$ TSP-d$_4$ as the internal chemical shift reference.

2.2. Wine samples

A total of 111 commercial New Zealand wines produced between 2019 and 2025 were selected for analysis. The sample set comprised Syrah ($n = 27$) and Pinot Noir ($n = 30$) as representative red wines, and Sauvignon Blanc ($n = 28$) and Chardonnay ($n = 26$) as representative white wines. Wines were purchased in March–April 2026 as 750 mL bottles from a retail vendor in Auckland, New Zealand, and retail prices were recorded in New Zealand dollars (NZD). Grape variety, vintage, and geographical origin were assigned according to the information displayed on the bottle labels and were not independently verified against producer records or certified reference samples. Consequently, the study evaluated discrimination and class membership relative to declared label information; it did not establish whether individual wines were counterfeit or mislabelled. Sample characteristics, including grape variety, vintage, retail price, and geographical origin (North, $n = 41$ or South Island, $n = 70$), are summarised in Table S1. This classification was adopted because the two islands have distinct viticultural environments that differ in climate, growing degree days, rainfall patterns, soil characteristics, and dominant grape varieties, all of which influence wine composition and regional typicity.

2.3. ^{1}H NMR metabolomic fingerprinting

2.3.1. Sample preparation and spectral acquisition

Before NMR analysis, wine samples were filtered through 0.45 μm nylon syringe filters to remove suspended particles. An aliquot of 1.8 mL of filtered wine was mixed with 0.2 mL of deuterated phosphate buffer (1 M KH_2PO_4 and 1 mM TSP-d$_4$ sodium salt in D_2O, containing 10 mg sodium azide per 100 mL) and homogenised thoroughly. The pH of each sample was adjusted to 3.10 ± 0.02 using a 1 M phosphoric acid solution

to minimise chemical shift variation among samples and improve spectral comparability. Following pH adjustment, the samples were transferred into 5 mm NMR tubes for spectroscopic acquisition. D_2O was used as the field-frequency lock solvent, while TSP-d_4 served as the internal chemical shift reference.

Proton nuclear magnetic resonance (^{1}H NMR) spectra were acquired using a Bruker Ascend™ 400 MHz spectrometer (Bruker BioSpin GmbH, Rheinstetten, Germany). A one-dimensional proton experiment with water suppression was employed using D_2O as the deuterated solvent. NMR data acquisition was performed using TopSpin version 5.0.0, whereas spectral processing and binning were performed using TopSpin version 4.2.0. The acquisition parameters were as follows: free induction decay (FID) size of 32,768 data points, relaxation delay of 5 s, 64 scans, pulse width of 13.6 μs, sample temperature at 25 °C, transmitter frequency offset of 1880.61 Hz, spectral width of 6393.86 Hz, and total acquisition time of approximately 9 min per sample.

2.3.2. Pre-processing of ^{1}H NMR data and principal component analysis (PCA)

Spectral processing was performed in TopSpin 4.2.0 (Bruker Biospin, Germany) and included exponential line broadening followed by Fourier transformation, zero- and first-order phase correction, and baseline correction. Spectral binning was conducted using a custom Python script executed within the TopSpin Jython environment. The processed ^{1}H NMR spectral region between 0.20 and 8.00 ppm was extracted from each spectrum and divided into fixed-width bins of 0.01 ppm. Regions corresponding to ethanol resonances (1.1385–1.1948 ppm and 3.6008–3.6745 ppm) and residual water/HOD signals (4.75–5.00 ppm) were excluded prior to binning. For each retained bin, only positive spectral intensity values were summed, while zero and negative values were omitted. To account for differences in overall signal intensity, total-area normalisation was applied independently to each spectrum by dividing the intensity of each retained bin by the sum of all retained bin intensities within that spectrum. Sample classes were assigned automatically based on the alphabetical prefix of the corresponding TopSpin sample name. The resulting dataset was exported as a comma-separated values (CSV) file containing sample identifiers, class labels, and normalised intensities for all retained spectral bins, yielding the final spectral-binning matrix used for chemometric and machine learning analyses.

For multivariate analysis, the ^{1}H NMR data matrix (111 wines, 740 spectral bins, totalling 82,140 data points) was normalised to total area, mean-centred, and autoscaled to unit variance. Variables with near-zero variance ($< 1 \times 10^{-15}$) were removed prior to analysis. Principal component analysis (PCA) was performed in Python (scikit-learn, NumPy, and SciPy) using full singular-value decomposition to explore the major sources of variation in the dataset. The PCA model was fitted exclusively to the spectral variables, and grape-variety and geographical-origin information were used only for post hoc interpretation of score plots. Group centroids and covariance-based 95% confidence ellipses were added to PC1-PC2, PC1-PC3, and PC2-PC3 projections. Component retention was evaluated using Horn's parallel analysis (1000 permutations), supported by the broken-stick criterion and cumulative explained variance. Model stability was assessed by bootstrap resampling (1000 iterations) with orthogonal Procrustes alignment, and stable high-contribution loading regions were grouped into contiguous 0.01-ppm intervals for interpretation.

2.4. Discrimination of wines using support vector machines (SVM)

SVM construct optimal decision boundaries, known as hyperplanes, to maximise separation between predefined classes and can model non-linear relationships effectively using kernel functions. In this study, SVM analysis was used as a supervised machine-learning approach to classify wines by geographical origin (North Island versus South Island), vintage, and varietal composition (Syrah, Pinot Noir, Chardonnay, and Sauvignon Blanc). The dataset was randomly partitioned into training (70%) and independent test (30%) subsets using a fixed random seed (1000). Models were developed using a radial basis function (RBF) kernel with $\gamma = 0.00135$. Model optimisation was performed using 10-fold cross-validation (seed = 1000) and grid-search tuning of the regularisation parameter (C) over the range 1–10. The SVM solver used a convergence tolerance of 0.001 and a maximum of 1000 iterations (Urtubia et al., 2021). All analyses were performed using TIBCO Statistica v.14.1.0.8 (TIBCO Software Inc., San Ramon, CA, USA).

2.5. Discrimination of wines using artificial neural networks (ANN) and automated network search (ANS)

ANN are supervised machine-learning algorithms capable of modelling complex linear and non-linear relationships between variables. ANS extends this approach by automatically generating and evaluating multiple network architectures to identify the optimal model for a given classification problem. In this study, ANN modelling was used as a supervised machine-learning approach to classify wines by geographical origin and varietal composition. The dataset was randomly divided into training (70%) and test and validation (20% and 10%, respectively) subsets. A fixed random seed of 1000 was used for dataset allocation and network initialisation to support reproducibility. A predefined multilayer perceptron (MLP) network architecture was first evaluated for geographical-origin and varietal classification. For geographical-origin classification, an MLP 740-25-2 architecture with 25 hidden neurons was employed, using the BFGS training algorithm, cross-entropy error function, hyperbolic tangent (tanh) hidden-layer activation, and softmax output activation. For varietal classification, an MLP 740-25-4 architecture with the same activation functions and error function was evaluated. ANS was then used to optimise network topology by automatically generating and evaluating 20 candidate MLP architectures with 8 to 25 hidden neurons. Both sum-of-squares (SOS) and cross-entropy error functions were considered during model development. The five best-performing networks were retained and compared according to their classification performance. The selected ANS architectures included MLP 740-24-2, MLP 740-20-2, MLP 740-15-2, MLP 740-8-2, MLP 740-21–4, MLP 740-23-4, MLP 740-18-4, and MLP 740-15-4 networks. All analyses were performed using TIBCO Statistica v.14.1.0.8 (TIBCO Software Inc., San Ramon CA, USA) (Cosme et al., 2021).

2.6. Discrimination of wines using random forest (RF)

RF is a supervised ensemble machine-learning method that combines multiple decision trees to perform classification and regression tasks. In this study, RF was applied to classify wines by geographical origin, vintage, and varietal composition. Classification models were developed using equal misclassification costs and estimated prior probabilities. Models were constructed using 60 trees, with 10 randomly selected predictors evaluated at each node, a random test-data proportion of 0.30, and a subsample proportion of 0.50. Tree growth was restricted to a maximum depth of 10, with minimum parent and child node sizes of five observations and a maximum of 100 nodes per tree. A random-number seed of 1 was used to ensure reproducibility. The advanced stopping condition was enabled, with the number of cycles used to calculate mean error set to 10 and the percentage decrease in training error set to 5%.

Variable-importance rankings were generated to identify the ten most influential spectral regions contributing to classification (Vacchina et al., 2026). To aid interpretation, the most important RF predictors were tentatively assigned to metabolite-associated spectral regions using published ^{1}H NMR chemical-shift data for wine metabolites (Hiniesta-Valero et al., 2025; Le Mao et al., 2021; Le Mao et al., 2024; Le Mao, Da Costa, & Richard, 2023; Lee et al., 2024). Because each predictor represented a 0.01-ppm spectral bucket and signal overlap is

inherent to wine matrices, these assignments were considered tentative and interpreted as metabolite-associated spectral regions rather than definitive identification of individual compounds. All analyses were performed using TIBCO Statistica v.14.1.0.8 (TIBCO Software Inc., San Ramon, CA, USA).

2.7. Authentication of wines using data driven - soft independent modelling of class analogy (DD-SIMCA)

DD-SIMCA was applied as a one-class classification (OCC) approach to evaluate the authenticity of individual wine varieties (Syrah, Pinot Noir, Chardonnay, and Sauvignon Blanc) using an $\alpha = 0.01$; the outlier threshold was calculated for $\gamma = 0.01$ (Kucheryavskiy et al., 2024). Unlike discriminant classification methods, which assign samples to one of several predefined classes, DD-SIMCA constructs a model using only samples from a single target class and assesses whether new samples belong to that class. Consequently, performance statistics are calculated relative to the target class. To avoid overly optimistic estimates of model performance, specificity was evaluated separately against each alternative class, and the class producing the lowest selectivity was considered the "nearest-of-kin" class. A separate DD-SIMCA model was developed for each wine variety using a four-step workflow. First, an initial DD-SIMCA model was constructed using all 740 NMR variables, and the optimal number of PCs was determined. Selectivity was calculated against each alternative varietal class to identify the nearest-of-kin class. Second, variable selection was performed using the Leave One Variable Excluded (LOVE) approach to improve model efficiency (Pomerantsev et al., 2025). A Procrustes Cross-Validation (PCV) set was employed to estimate model sensitivity, and the nearest-of-kin class to evaluate specificity. Third, a refined DD-SIMCA model was developed using only the selected variables, and the optimal number of PCs was re-evaluated. Because the selected variables depended on the target class, a different subset of variables was obtained for each wine variety. Finally, the optimised model was challenged with all alternative classes to determine the final figures of merit, including sensitivity, specificity, and selectivity. The analysis was performed using the mda-tools software (https://mda.tools/).

2.8. Discrimination of wines using multiclass partial least squares – discriminant analysis (PLS-DA)

Multiclass PLS-DA was applied in the soft and hard versions to discriminate among all wine varieties (Pomerantsev & Rodionova, 2018). The PCV method (random split into five segments) was used for optimisation and validation. The number of latent variables (LVs) was selected based on a trade-off between the mean class efficiency (TEFF) values obtained for the training and test (e.g., PCV) datasets. In the soft version, the significance level of $\alpha = 0.02$ was selected using the Receiver Operating Characteristic (ROC) approach. The calculations were performed using the PLS-DA – MATLAB GUI tool (https://github.com/yzontov/pls-da/releases) and the Chemometric add-in for Excel (Microsoft Excel, Microsoft Corp., Redmond, WA, USA) for classification assessment and feature evaluation.

2.9. Discrimination of geographical origin of wines using soft binary partial least squares – discriminant analysis (SB PLS-DA)

Soft Binary Partial Least Squares – Discriminant Analysis (SB PLS-DA) method is a probabilistic discriminator that focuses on the individual characteristics of each sample involved in discrimination (Pomerantsev & Rodionova, 2026). SB PLS-DA was used to discriminate between the geographical origin (North Island and South Island) of wines. The PCV method (random split into five segments) was used for optimisation and validation. The number of LVs was selected based on a trade-off between the total efficiency values obtained for the training and test (PCV) datasets. The significance level of $\alpha = 0.02$ was selected using the ROC approach. The analysis was performed using the mda-tools software (https://mda.tools/).

2.10. Classification performance indices of chemometric and machine learning algorithms and statistical analysis

Classification performance was evaluated using confusion matrices. Unless otherwise stated, the confusion matrices and associated performance metrics correspond to the final classification results generated by each modelling approach and include predictions from both the training and test subsets. These metrics describe classification performance across the full dataset rather than performance on the test subset alone. Model performance was assessed using sensitivity, specificity, precision, accuracy, and Matthews correlation coefficient (MCC).

For geographical-origin classification using SVM, RF, and ANN/ANS, North Island was designated as the positive class and South Island as the negative class. For varietal classification, these metrics were first calculated separately for Chardonnay, Pinot Noir, Syrah, and Sauvignon Blanc using a one-versus-rest approach. Mean class performance was subsequently obtained by averaging the corresponding metrics across the four varietal classes. Overall multiclass accuracy was independently calculated from the confusion matrix as the proportion of correctly classified samples relative to the total number of samples. Sensitivity, specificity, precision, and accuracy were calculated according to Eqs. (1)–(4), respectively, where TP, TN, FP, and FN represent true positives, true negatives, false positives, and false negatives (Sokolova & Lapalme, 2009).

$$\text{Sensitivity} = \text{TP}/(\text{TP} + \text{FN}) \tag{1}$$

$$\text{Specificity} = \text{TN}/(\text{TN} + \text{FP}) \tag{2}$$

$$\text{Precision} = \text{TP}/(\text{TP} + \text{FP}) \tag{3}$$

$$\text{Accuracy} = (\text{TP} + \text{TN})/(\text{TP} + \text{TN} + \text{FP} + \text{FN}) \tag{4}$$

MCC was used as a balanced measure of classification performance because it incorporates all elements of the confusion matrix (TP, TN, FP, and FN) and is less sensitive to class imbalance than accuracy alone. MCC was calculated according to Eq. (5). For varietal classification, MCC was first calculated separately for each wine variety using a one-versus-rest approach and subsequently averaged across wine varieties. MCC ranges from −1 to +1, where +1 indicates perfect agreement, 0 indicates performance equivalent to random classification, and −1 indicates complete disagreement between observations and predictions (Chicco & Jurman, 2020):

$$MCC = \frac{(TP\ x\ TN) - (FP\ x\ FN)}{\sqrt{(TP + FP)(TP + FN)(TN + FP)(TN + FN)}} \tag{5}$$

Wine prices were expressed as the average ± standard deviation and were compared according to geographical origin (North Island, $n = 41$; South Island, $n = 70$) and grape variety (Chardonnay, $n = 26$; Pinot Noir, $n = 30$; Syrah, $n = 27$; Sauvignon Blanc, $n = 28$). For comparisons involving two groups (e.g., North and South Island), differences were assessed using an unpaired Student's *t*-test. Comparisons among wine varieties were performed using one-way analysis of variance (ANOVA), followed by Tukey's test when significant differences were detected. Homogeneity of variances was evaluated using the Brown-Forsythe test. Statistical significance was established at $p < 0.05$. Statistical analyses and graphical representations were performed using GraphPad Prism v.8 (GraphPad Software, Boston, MA, USA).

3. Results and discussion

3.1. General characterisation of wines using untargeted ^{1}H NMR metabolomics

Representative ^{1}H NMR spectra of New Zealand Chardonnay, Sauvignon Blanc, Pinot Noir, and Syrah wines are shown in Fig. 1a. Ethanol and glycerol resonances dominate the spectra and partially obscure lower-intensity signals; therefore, several expanded spectral regions (0.8–1.5, 1.5–2.6, 2.6–3.4, 3.4–3.9, 3.9–4.7, 5.0–6.2, and 6.2–8.5 ppm) were examined in detail according to published wine metabolomics studies (Hiniesta-Valero et al., 2025; Le Mao et al., 2024; Le Mao, Da Costa, & Richard, 2023; Lee et al., 2024; Leleu et al., 2026). Fig. 1b shows the expanded 0.8–1.5 ppm region, where the ethanol methyl

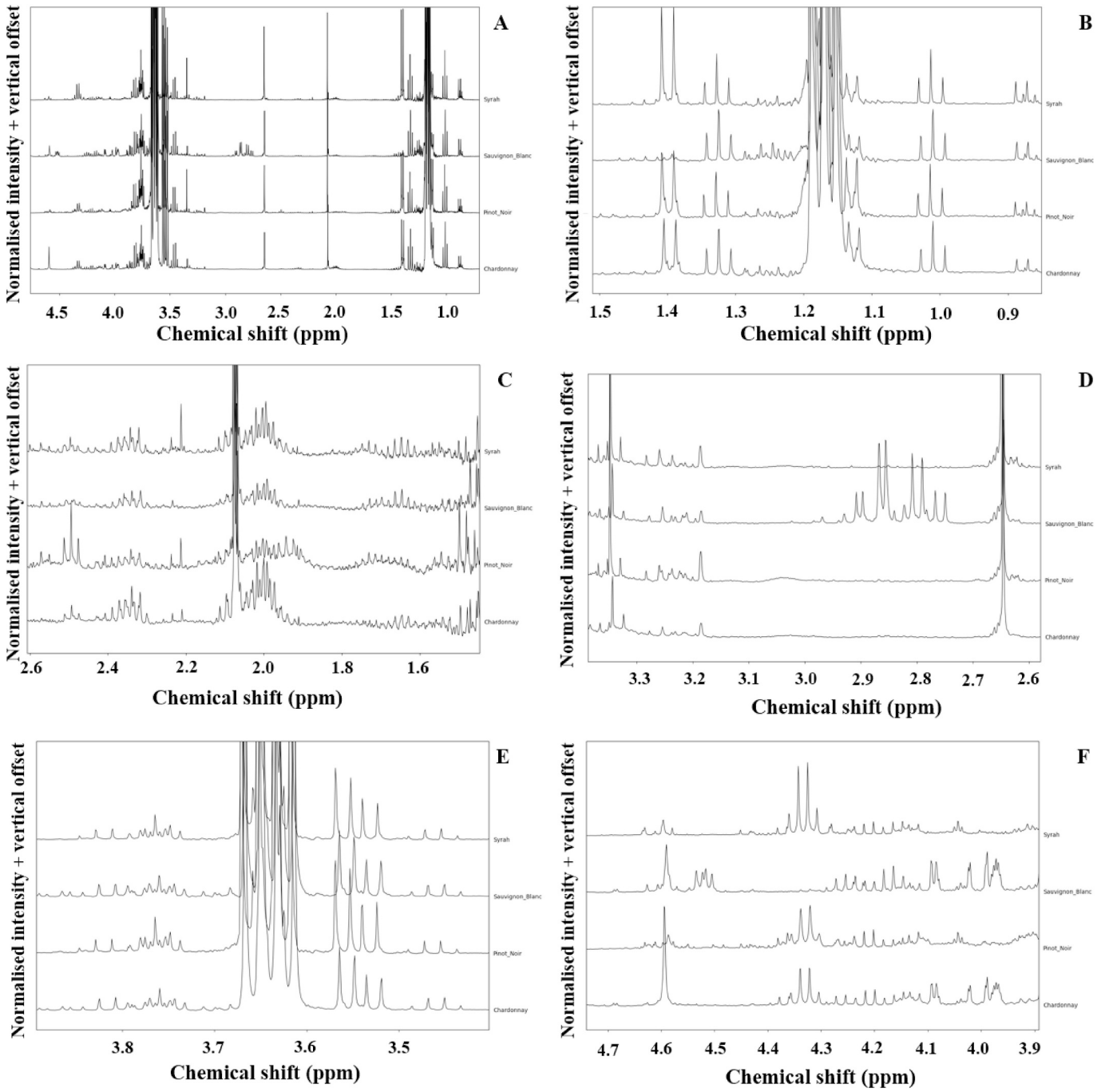


Fig. 1. Representative stacked ^{1}H NMR spectra of Chardonnay, Pinot Noir, Sauvignon Blanc, and Syrah wines. (A) Overview spectrum (0.5–4.8 ppm); traces are vertically offset for visual comparison. Ethanol and glycerol resonances dominate the spectra. Expanded spectral regions: (B) 0.8–1.5 ppm, containing ethanol, higher alcohols, amino acids, and fermentation-derived metabolites; (C) 1.5–2.6 ppm, dominated by organic acids, amino acids, and fermentation products; (D) 2.6–3.4 ppm, containing organic acids, choline-related compounds, carbohydrates, and phenolic-associated resonances; (E) 3.4–3.9 ppm, dominated by glycerol, ethanol, carbohydrates, and polyols; (F) 3.9–4.7 ppm, containing carbohydrates, organic acids, and fermentation-derived metabolites; (G) 5.0–6.2 ppm, including anomeric sugar resonances and flavanol-associated signals; and (H) 6.2–8.5 ppm, corresponding primarily to aromatic and phenolic metabolites. Peak assignments were based on published wine ^{1}H NMR literature and should be regarded as tentative because of spectral overlap among metabolites. ^{1}H NMR spectra were exported from the analysis software and formatted in Microsoft PowerPoint for publication-quality presentation, including adjustment of font sizes and panel layouts.

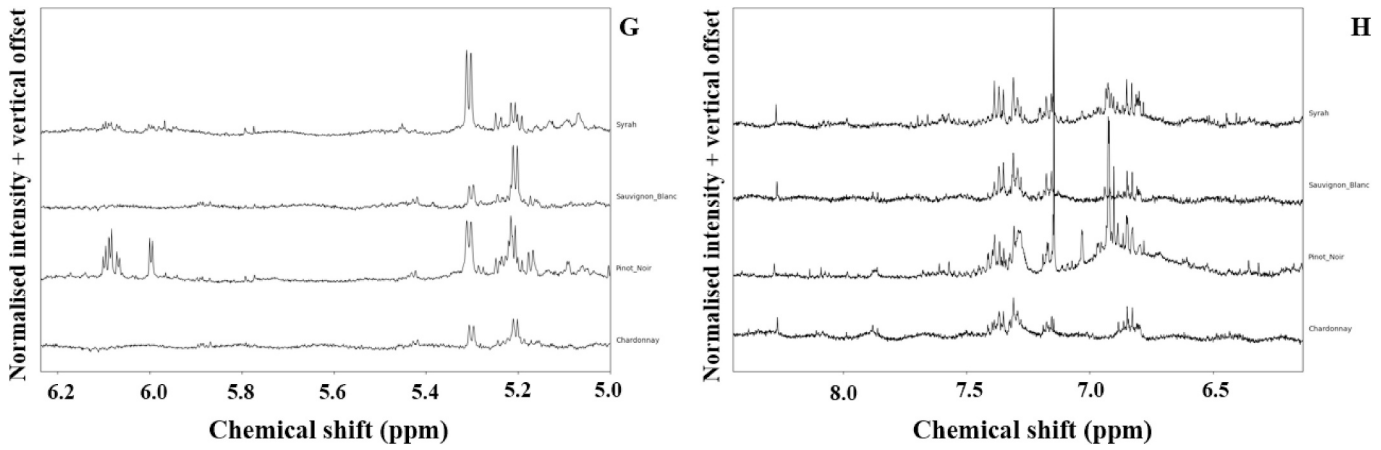


Fig. 1. (*continued*).

triplet (~1.18 ppm) dominates the spectrum. Additional resonances arise from branched-chain amino acids (valine, leucine and isoleucine at around 0.94–1.04 ppm), fermentation-derived metabolites such as 2,3-butanediol at 1.13 ppm, acetoin at near 1.37 ppm, ethyl lactate and lactic acid at near 1.40–1.42 ppm, as well as amino acids including alanine at near 1.50 ppm and threonine at near 1.33 ppm (Du et al., 2007; Le Mao et al., 2024; Le Mao, Da Costa, & Richard, 2023). Although the overall spectral patterns were similar among varieties, signal intensities differed in regions associated with fermentation products and organic acids (Ali et al., 2011; Le Mao et al., 2024; Le Mao, Da Costa, & Richard, 2023; López-Rituerto et al., 2009).

Fig. 1c shows the expanded 1.5–2.6 ppm region for the four wine varieties. The intense resonance at approximately 2.07–2.08 ppm corresponds to an acetyl-rich region, where acetic acid and ethyl acetate contribute prominent singlets (Le Mao et al., 2024; Le Mao, Da Costa, & Richard, 2023; Leleu et al., 2026). Additional signals arise from amino acids and fermentation-derived metabolites, including proline (1.99–2.35 ppm), acetoin (~2.20 ppm), pyruvate (~2.35 ppm), glutamate/glutamine (~2.13–2.14 and 2.41–2.42 ppm), and GABA (~2.42 ppm) (Ali et al., 2011; Du et al., 2007; García-Aguilera et al., 2023; Le Mao, Da Costa, & Richard, 2023). Catechin may also contribute to the signal observed around 2.55–2.56 ppm (Le Mao, Da Costa, & Richard, 2023). Visible differences in signal intensity among wine varieties suggest variation in the abundance of amino-acid- and fermentation-related metabolites.

Fig. 1d shows the expanded 2.6–3.4 ppm region, which is dominated by resonances from organic acids, carbohydrates, and choline-related compounds. A well-resolved succinate singlet is observed at approximately 2.65–2.66 ppm (Du et al., 2007; Le Mao et al., 2024; Leleu et al., 2026), while malate and citrate contribute overlapping signals between 2.78 and 3.00 ppm (Du et al., 2007; Le Mao, Da Costa, & Richard, 2023). Additional overlap from epicatechin (~2.76/2.90) and shikimate (~2.75) occurs within this interval, highlighting the region's chemical complexity (Le Mao, Da Costa, & Richard, 2023). Choline, assigned to the resonance at approximately 3.19 ppm, represents one of the most reliable metabolite assignments in the spectrum, whereas glucose and arginine contribute to signals near 3.23 ppm (Le Mao et al., 2024; Le Mao, Da Costa, & Richard, 2023). Noticeable differences among wine varieties are observed in the 2.7–3.0 ppm range, suggesting variation in organic-acid and aromatic-metabolite composition.

Fig. 1e shows the expanded 3.4–3.9 ppm region, which is dominated by resonances from carbohydrates, glycerol, and other oxygenated metabolites. Glycerol is a major contributor, with characteristic signals reported at approximately 3.55, 3.64–3.66, and 3.77–3.78 ppm, partially overlapping with ethanol and carbohydrate resonances (Du et al., 2007; Hiniesta-Valero et al., 2025; Le Mao, Da Costa, & Richard, 2023). This region also shows additional contributions from fructose, arabinose, xylose, mannitol, phenethyl alcohol, arginine, alanine, and tyrosol (Le Mao, Da Costa, & Richard, 2023). Although the overall spectral profiles are similar across wine varieties, signal intensities differ noticeably, particularly for resonances associated with glycerol and carbohydrate-derived metabolites. These compounds are influenced by grape composition, fermentation processes, and wine maturation, making this region relevant for varietal discrimination.

Fig. 1f shows the expanded 3.9–4.7 ppm region, which contains resonances associated with ethyl acetate, ethyl lactate, organic acids, carbohydrates, and other oxygenated metabolites. Characteristic signals include ethyl acetate (~4.12 ppm), ethyl lactate (~4.27 ppm), malate (~4.53 ppm), tartrate (~4.60 ppm), and β-glucose (~4.63 ppm) (Du et al., 2007;Le Mao et al., 2024; Le Mao, Da Costa, & Richard, 2023; Leleu et al., 2026). Additional overlap from catechin (~4.15 ppm) and other secondary metabolites contributes to the complexity of this region. Compared with the other wine varieties, Sauvignon Blanc exhibits more intense signals between approximately 4.50 and 4.65 ppm: arabinose (~4.50 ppm), malate-related oxygenated protons, glucose (~4.55 ppm, d), sucrose (~4.57 ppm, d) and tartrate near ~4.60 ppm (García-Aguilera et al., 2023; Le Mao, Da Costa, & Richard, 2023). Variability is also observed in the 4.1–4.4 ppm interval, which contains contributions from lactate-, acetoin-, and ethyl-lactate-associated resonances. The observed differences indicate variation in sugar-, organic-acid-, and fermentation-associated spectral regions, although overlapping signals prevent definitive metabolite assignments.

Fig. 1g shows the expanded 5.0–6.2 ppm region. The prominent signals near 5.2–5.3 ppm are consistent with anomeric sugar and uronic acid resonances, including α-glucose (~5.22–5.23 ppm) and galacturonic acid (~5.30–5.32 ppm), both previously reported in wine metabolomic studies (Le Mao et al., 2024;Le Mao, Da Costa, & Richard, 2023; Leleu et al., 2026). The 5.99–6.10 ppm region is of particular interest because (+)-catechin and (−)-epicatechin have multiple validated meta-coupled aromatic resonances in this interval (Le Mao, Da Costa, & Richard, 2023; Leleu et al., 2026). The four wine varieties show differences in spectral fine structure, particularly for Pinot Noir, suggesting variation in flavanol-associated metabolites. However, spectral overlap in this region prevents unambiguous distinction between (+)-catechin and (−)-epicatechin; therefore, these signals are better interpreted as flavanol-related resonances (Ali et al., 2011; Le Mao, Da Costa, & Richard, 2023).

Fig. 1h shows the expanded 6.2–8.5 ppm region, which contains numerous aromatic and phenolic metabolites associated with grape variety, vintage, and wine composition. Previous metabolomics studies have identified (+)-catechin, (−)-epicatechin, gallic acid, caffeic acid, amino acids, and other aromatic metabolites as important contributors to wine differentiation (Le Mao, Da Costa, & Richard, 2023). The wine varieties differ clearly, with Pinot Noir and Syrah showing greater

aromatic complexity and signal density than the white wines. This contrast aligns with the higher extraction of skin- and seed-derived phenolics typically associated with red-wine production, although the spectra should not be interpreted as quantitative measurements of phenolic concentration. Several RF-important regions identified later in the study occur within this aromatic window, notably 6.91–6.93 ppm, 7.03–7.05 ppm, and 7.30–7.31 ppm. The first two regions are consistent with flavanol-associated resonances, whereas the latter appears to represent an overlap involving phenethyl alcohol, phenylalanine, and other aromatic metabolites.

^{1}H NMR spectra of New Zealand red and white wines show differences among varieties in regions associated with organic acids, amino acids, carbohydrates, fermentation products, and phenolic compounds. The observed spectral differences therefore provide a chemical basis for investigating wine classification, but do not establish which factors (e.g., chemical compounds) produced those differences.

3.2. PCA analysis

PCA provided an unsupervised overview of the intrinsic structure of the ^{1}H NMR fingerprints before applying supervised classification approaches. The first three principal components explained 17.4%, 15.7%, and 13.3% of the total standardised spectral variance, respectively, for a cumulative 46.4%. Post hoc annotation of the fixed PCA scores by grape variety revealed a clear, broad organisation of the samples, particularly in the PC1–PC3 projection, although the four varietals were not completely separated (Fig. 2a). Pinot Noir and Syrah occupied largely overlapping regions of the score space, while Chardonnay and Sauvignon Blanc also showed partial overlap. Thus, the dominant unsupervised variation contained varietal-related structure but was not sufficient to fully separate the four varietal groups. Similar studies have demonstrated that ^{1}H NMR fingerprints capture grape-dependent compositional differences involving organic acids, amino acids, sugars and phenolic metabolites, although the degree of PCA separation varies with the varieties and sample population (Ehlers et al., 2022; Le Mao, Da Costa, Bautista, et al., 2023; Mascellani et al., 2021; Son et al., 2009).

Annotation of the same PCA coordinates by geographical origin showed extensive overlap between North and South Island wines, with only a modest displacement mainly along PC1 and little separation in the PC2–PC3 projection (Fig. 2b). This suggests that island-level provenance was not a dominant source of variation captured by the leading PCs. The weak separation may partly reflect the broad North/South grouping, which encompasses heterogeneous growing areas, grape varieties and winemaking-related compositional variation that may obscure subtler regional effects. Because PCA identifies directions of maximum overall variance rather than those that maximise class separation, provenance-related information may remain distributed across lower-variance spectral dimensions. Previous ^{1}H NMR studies have similarly shown that unsupervised PCA can reveal weak or incomplete geographical structure, while region-related metabolic differences remain detectable (Crook et al., 2021; Gougeon et al., 2019).

Permutation-based parallel analysis indicated that 13 PCs contained more variance than expected under the randomised reference distribution (Fig. S1), confirming that the spectral structure extended beyond the first few PCs. Nevertheless, PC1–PC3 together accounted for 46.4% of the total standardised variance and showed greater bootstrap stability

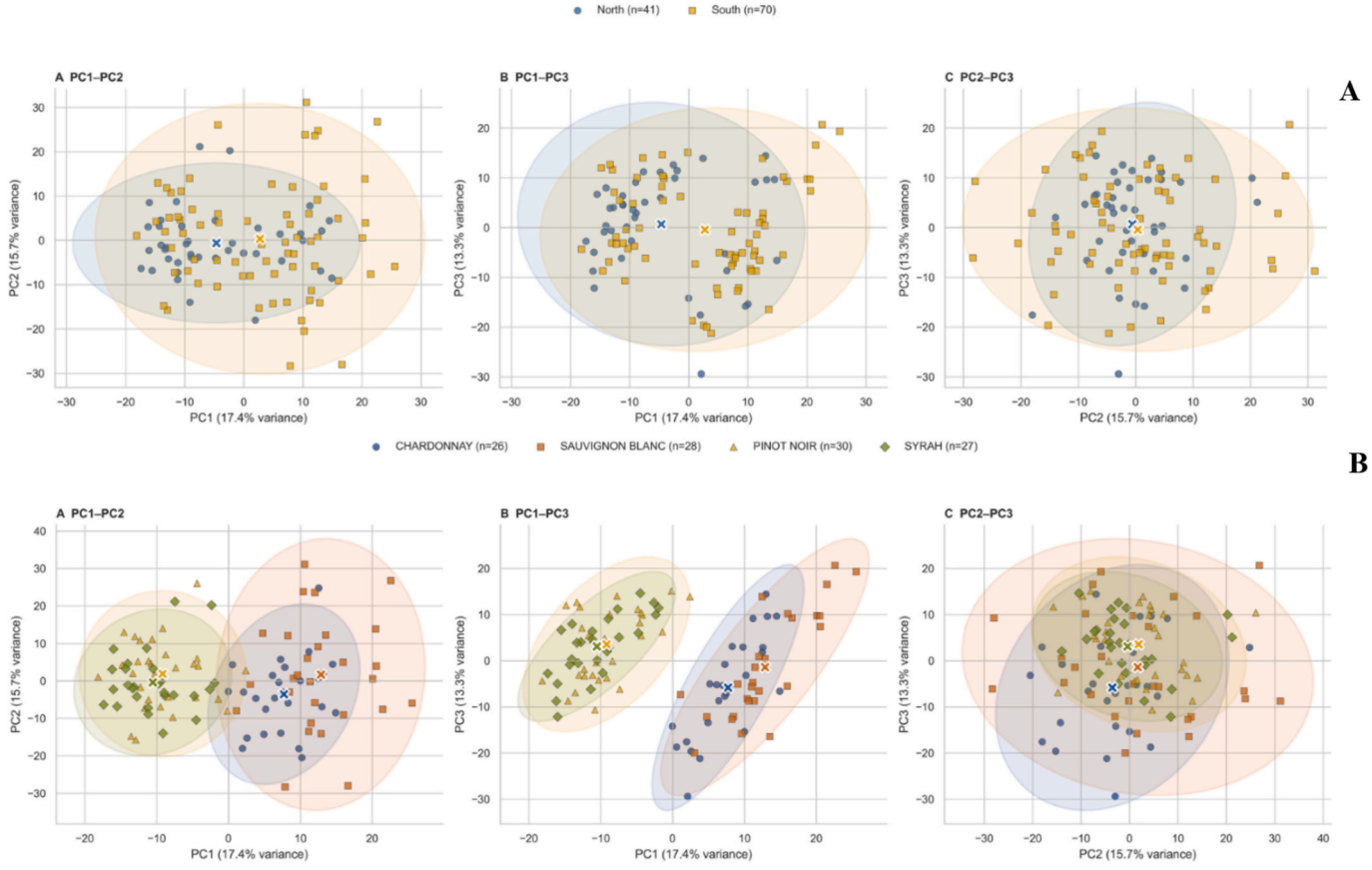


Fig. 2. Unsupervised Principal Component Analysis (PCA) score structure of the ^{1}H NMR wine fingerprints annotated by geographical origin (A) and varietal (B). Grape-variety labels (Chardonnay, Sauvignon Blanc, Pinot Noir and Syrah), group centroids (×) and covariance-based 95% within-group score-dispersion ellipses were added post hoc to the fixed PCA coordinates. The percentages shown on the axes indicate the proportion of total standardised spectral variance explained by each principal component. Panels A–C show PC1–PC2, PC1–PC3 and PC2–PC3 score projections, respectively. Crosses indicate group centroids and ellipses represent covariance-based 95% within-group score dispersion.

than the broader retained PCA subspace, supporting their use for detailed interpretation. Parallel analysis is preferable to selecting components solely from an arbitrary cumulative-variance threshold because it evaluates observed eigenvalues against those expected from randomised data (Vitale & Saccenti, 2018). Bootstrap-supported loadings showed that the principal variation was distributed across several NMR regions rather than driven by a single resonance. Bootstrap resampling provides an additional assessment of the stability of PCA loadings (Babamoradi et al., 2013). Given the signal overlap characteristic of one-dimensional wine ^{1}H NMR spectra, these loading regions were interpreted as reproducible spectral intervals rather than assigned to individual metabolites (Viskić et al., 2021).

3.3. Classification of wines using SVM

The SVM model showed moderate performance for geographical origin classification and excellent performance for varietal discrimination of New Zealand wines (Table 1a). The model classified geographical origin with 82.9% accuracy and an MCC of 0.635, misclassifying only two South Island wines as North Island wines, while 17 North Island wines were incorrectly assigned to the South Island group (Table 1b). Comparable results have been reported for wine authentication studies based on spectroscopic fingerprints. For example, varietal classification accuracies exceeding 80% were obtained for 403 Hungarian wines (Chardonnay, Sauvignon Blanc, Riesling, Cabernet Franc, Merlot, and Blaufränkisch) using ^{1}H NMR data and Extreme Gradient Boosting (Barátossy et al., 2021), while a combination of ^{1}H NMR, FT-Raman spectroscopy and SVM achieved accuracies of 96% and 98% for varietal and geographical origin classification, respectively, in a set of 50 Romanian wines (Hategan et al., 2024). However, the latter study used a substantially smaller dataset, which may reduce the model's generalisability.

Table 1
Performance of Support Vector Machine (SVM) classification models for geographical origin and varietal discrimination of New Zealand wines.

(a) Classification indices

Classification task	Accuracy (%)	Sensitivity (%)	Specificity (%)	Precision (%)	MCC
Geographical origin	82.9	58.5	97.1	92.3	0.635
Varietal (mean class-specific one-versus-rest metrics)[a]	97.7	95.6	98.5	95.8	0.942
Chardonnay	96.4	100.0	95.3	86.7	0.909
Pinot Noir	99.1	96.7	100.0	100.0	0.977
Syrah	99.1	100.0	98.8	96.4	0.976
Sauvignon Blanc	96.4	85.7	100.0	100.0	0.904

(b) Confusion matrix – Geographical origin

Actual/Predicted	North	South
North	**24**	17
South	2	**68**

(c) Confusion matrix – Varietal

Actual/Predicted	Chardonnay	Pinot Noir	Syrah	Sauvignon Blanc
Chardonnay	**26**	0	0	0
Pinot Noir	0	**29**	1	0
Syrah	0	0	**27**	0
Sauvignon Blanc	4	0	0	**24**

(d) Confusion matrix – Vintage

Actual/Predicted	2019	2020	2021	2022	2023	2024	2025
2019	**0**	0	0	4	0	1	0
2020	0	**0**	0	7	1	1	0
2021	0	0	**2**	7	0	4	0
2022	0	0	0	**13**	6	1	0
2023	0	0	0	7	**15**	8	0
2024	0	0	0	3	5	**19**	0
2025	0	0	0	0	3	4	**0**

Note (a): MCC, Matthews correlation coefficient; sensitivity = TP/(TP + FN); specificity = TN/(TN + FP); precision = TP/(TP + FP); accuracy = (TP + TN)/(TP + TN + FP + FN). [a] For varietal classification, sensitivity, specificity, precision, accuracy, and MCC were calculated separately for Chardonnay, Pinot Noir, Syrah, and Sauvignon Blanc using a one-versus-rest approach and subsequently averaged across classes. The overall multiclass accuracy derived from the confusion matrix was 95.5% (106/111 correctly classified samples).
Note (c): Rows represent actual classes and columns represent predicted classes.
Note (d): The overall multiclass accuracy derived from the confusion matrix was 44.1% (49/111 correctly classified samples).

In contrast, varietal discrimination achieved a mean one-versus-rest accuracy of 97.7%, sensitivity of 95.6%, specificity of 98.5%, precision of 95.8%, and MCC of 0.942, corresponding to an overall multiclass accuracy of 95.5% (106/111 correctly classified samples). Pinot Noir and Syrah showed the highest individual performance, both reaching 99.1% accuracy with MCC values of 0.977 and 0.976, respectively, while Chardonnay and Sauvignon Blanc achieved 96.4% accuracy with MCC values of 0.909 and 0.904, respectively. Misclassification was limited to four Sauvignon Blanc wines classified as Chardonnay and one Pinot Noir wine classified as Syrah (Table 1c). The overlap between Chardonnay and Sauvignon Blanc is consistent with metabolomics studies reporting similarities in the non-volatile composition of these white wine varieties despite successful discrimination using multivariate approaches (Khakimov et al., 2022). The SVM classification performance further supports previous reports that machine-learning models can successfully extract provenance-related information from wine chemistry. For example, soft-sensor approaches developed for New Zealand Pinot Noir based on the phenolic composition demonstrated that a limited number of chemical parameters were sufficient to predict provenance, vintage, and price categories with accuracies exceeding 75%, highlighting the significant relationship between chemical composition and wine origin (An & Liu, 2026).

Because MCC provides a balanced evaluation of multiclass classification performance, greater emphasis was placed on MCC than on accuracy alone (Gorodkin, 2004). All models in Table 1 achieved MCC values above 0.600, indicating moderate to excellent agreement between observed and predicted classes. Varietal classification performed markedly better (MCC = 0.904–0.977) than geographical origin discrimination (MCC = 0.635), suggesting that the fingerprints supported more successful varietal classification in this dataset. Given the moderate dataset size (n = 111), with approximately 26–30 wines per varietal class, the high MCC values suggest that chemical differences captured by the ^{1}H NMR fingerprints, rather than class prevalence alone, drove classification performance. Future metabolomics studies should identify the specific compounds that differentiate wines from the North and South Islands.

Vintage may influence wine composition and potentially affect NMR-based classification. However, the SVM results (Table 1d) showed that vintage discrimination under the modelling conditions used was less successful than varietal or geographical-origin classification, achieving an overall accuracy of 44.1%. All wines from the 2019, 2020, and 2025 vintages were misclassified, with predictions concentrated in the 2022–2024 classes. These results indicate limited vintage discrimination under the modelling conditions used. Other wine metabolomics studies have reported vintage-associated differences (Roullier-Gall et al., 2016), highlighting the potential contribution of vintage- and maturation-related changes to wine fingerprints. Consequently, the lower vintage-classification accuracies observed here do not indicate that vintage had negligible influence on varietal or geographical-origin discrimination.

The significant price differences observed between geographical origins and grape varieties (Fig. S2a,b) provide further evidence that the sampled wines represent distinct commercial segments. North Island wines had higher average prices than South Island wines, while Syrah

had the highest average price and one of the best classification performances (MCC = 0.976). However, Pinot Noir achieved a similarly high MCC (0.977) despite a lower average price, indicating that market value alone does not explain classification success. Nevertheless, because the wines were selected for market availability and convenience, the observed price distributions reflect the sampled dataset rather than the New Zealand wine market.

3.4. Classification of wines using ANN and ANS

The ANN and ANS models showed variable performance in classifying New Zealand wines by geographical origin (Table 2a). The conventional ANN architecture (MLP 740-25-2) achieved an accuracy of 77.5% and an MCC of 0.519, correctly classifying 29 of 41 North Island wines and 57 of 70 South Island wines (Table 2b). Among the ANS-generated models, performance ranged from moderate (accuracy = 89.2%; MCC = 0.771) to moderate-high (accuracy = 93.7%; MCC = 0.864). The best-performing architecture, ANS MLP 740-24-2, correctly classified 36 North Island and 68 South Island wines, resulting in a sensitivity of 87.8%, specificity of 97.1%, precision of 94.7%, and an accuracy of 93.7%. The model assigned five North Island wines to the South Island class and two South Island wines to the North Island class.

For varietal discrimination, both ANN and ANS models achieved excellent classification performance, confirming that ^{1}H NMR fingerprints can capture variety-specific compositional signatures (Table 2c-j). The conventional ANN architecture (MLP 740-25-4) correctly classified 106 of 111 wines, achieving an overall multiclass accuracy of 95.5%. Its mean one-versus-rest accuracy was 97.8%, and its mean class-specific MCC was 0.940 (Table 2c,d). Chardonnay and Sauvignon Blanc showed the highest class-specific performance, each achieving 98.2% one-versus-rest accuracy, with MCC values of 0.950 and 0.952, respectively. Three misclassifications occurred between the red wine varieties: two Pinot Noir wines were classified as Syrah, and one Syrah wine was classified as Pinot Noir.

The ANS-generated architectures showed variable varietal classification performance. The best-performing ANS model, MLP 740-21–4, correctly classified 110 of 111 wines, achieving an overall multiclass accuracy of 99.1%. Its mean one-versus-rest accuracy was 99.5%, and its mean class-specific MCC was 0.988 (Table 2e,f). Likewise, ANS MLP 740-23-4 (overall multiclass accuracy = 97.3%; mean class-specific MCC = 0.964), had only three misclassified samples: one Chardonnay incorrectly assigned to Sauvignon Blanc, one Sauvignon Blanc classified as Chardonnay, and one Syrah classified as Sauvignon Blanc (Table 2g, h). ANS MLP 740-18-4 and MLP 740-15-4 produced identical confusion matrices, achieving 91.9% overall multiclass accuracy (102/111 correctly classified samples) and a mean class-specific MCC of 0.893. Errors included three Sauvignon Blanc wines misclassified as Chardonnay, one Chardonnay misclassified as Sauvignon Blanc, four Syrah wines misclassified as Pinot Noir, and one Pinot Noir misclassified as Syrah (Table 2i,j).

For comparison, (Jagatić Korenika et al., 2024) reported 88% classification accuracy for 34 Croatian sparkling wines using DOSY-NMR and ICP-MS data coupled with ANN. Although the sample populations and classification tasks differ, that study and previous reports illustrate the application of NMR fingerprints to wine classification (Bambina et al., 2024; Hategan et al., 2024; Viskić et al., 2021). In the present study, mean class-specific MCC values for varietal classification ranged from 0.893 to 0.988. MLP 740-21–4 achieved the highest performance, although automated network search did not improve all architectures relative to the predefined ANN.

3.5. Classification of wines using RF

As shown in Table 3a, RF performed differently for geographical-origin and varietal classification. Geographical-origin discrimination achieved 78.4% accuracy and an MCC of 0.544, indicating moderate predictive capability. The confusion matrix (Table 3b) revealed a bias toward South Island wines, with 69 of 70 samples correctly classified, whereas the model correctly identified only 18 of 41 North Island wines. Consequently, the model assigned 23 North Island wines to the South Island class, resulting in high specificity (98.6%) but relatively low sensitivity (43.9%). The reputation of South Island wines may reflect coherent, terroir-driven compositional signatures, particularly in Marlborough, where soil, climate, and vineyard-performance variables generate distinct regional patterns (Bramley et al., 2023). Similarly, previous studies have shown that regional provenance is embedded in the chemical composition of New Zealand Pinot Noir wines and can be recovered through multivariate analysis (Su et al., 2025). Therefore, the lower sensitivity for North Island wines may reflect greater compositional heterogeneity among northern production regions rather than an absence of regional chemical signatures. Future studies should analyse more North Island samples to explore these chemical differences.

Tentative assignment of the most influential RF predictors indicated that geographical-origin discrimination was driven primarily by spectral regions associated with amino acids, carbohydrates, organic acids, choline-related metabolites and aromatic phenolics (Table S2). These metabolite classes are affected by environmental conditions, grape maturity and fermentation processes, suggesting that RF captured broad terroir-related differences rather than relying on individual marker compounds. Because each predictor represented a 0.01-ppm bucket, multiple metabolites may contribute to a given signal; therefore, the assignments should be considered provisional and require confirmation through targeted metabolomics using standards and/or two-dimensional NMR experiments.

RF achieved a mean one-versus-rest accuracy of 96.0% and a mean class-specific MCC of 0.893 for varietal discrimination (Table 3a). Overall multiclass accuracy was 91.9%, corresponding to 102 correctly classified wines out of 111. Pinot Noir and Syrah performed best (98.2% accuracy; MCC > 0.950), whereas Chardonnay and Sauvignon Blanc had lower accuracy (93.7%) (Table 3c). Six Chardonnay wines were misclassified as Sauvignon Blanc, and one Sauvignon Blanc was misclassified as Chardonnay. Despite some overlap between Chardonnay and Sauvignon Blanc, the high specificity (92.8–98.8%) and MCC values (0.819–0.954) demonstrate that RF effectively captured grape variety-specific information within the ^{1}H NMR fingerprints. This pattern suggests greater compositional overlap between the two white wine varieties, consistent with previous GC–MS studies showing that Chardonnay and Sauvignon Blanc share many non-volatile metabolites and differ primarily in their relative abundances (Khakimov et al., 2022). Previous studies show that New Zealand Sauvignon Blanc wines have distinct regional chemical signatures that spectroscopic techniques can differentiate, and that geographical origin influences Sauvignon Blanc composition (Green et al., 2011). These environmental influences can increase within-variety heterogeneity, potentially reducing varietal separability compared with red wine varieties such as Pinot Noir and Syrah, which showed near-perfect classification performance.

Variable-importance analysis indicated that varietal differentiation was associated mainly with organic-acid, carbohydrate and aromatic/phenolic regions (Table S3). The prominence of phenolic-associated resonances among the highest-ranking predictors is consistent with the role of secondary metabolites in defining varietal characteristics. This may explain the higher classification performance for varietal than for geographical-origin discrimination.

Random Forest classification in Table 3d, using vintage as the response variable, achieved an overall accuracy of 48.6%, slightly higher than SVM (44.1%; Table 1d). Nevertheless, overlap among vintages was observed, with most wines being assigned to the 2022–2024 classes. Wines from the 2019, 2020, 2021, and 2025 vintages showed poor discrimination. These results do not establish whether vintage confounded varietal or geographical-origin classification. Vintage was unevenly distributed across grape varieties and geographical origins

Table 2
Performance of Artificial Neural Network (ANN) and Automated Network Search (ANS) -generated classification models for geographical origin and varietal discrimination of New Zealand wines.

(a) Geographical origin

Network Architecture	Accuracy (%)	Sensitivity (%)	Specificity (%)	Precision (%)	MCC	Training algorithm	Error function	Hidden activation	Output activation
ANS MLP 740-24-2	93.7	87.8	97.1	94.7	0.864	BFGS 22	SOS	Exponential	Tanh
ANS MLP 740-20-2	91.0	82.9	95.7	91.9	0.805	BFGS 15	SOS	Identity	Identity
ANS MLP 740-15-2	91.0	82.9	95.7	91.9	0.805	BFGS 25	SOS	Exponential	Exponential
ANS MLP 740-8-2	89.2	87.8	90.0	83.7	0.771	BFGS 19	SOS	Exponential	Tanh
ANN MLP 740-25-2	77.5	70.7	81.4	69.0	0.519	BFGS 4	Entropy	Tanh	Softmax

(b) Confusion matrix – Geographical origin

Model	Actual/Predicted	North	South
ANN MLP 740-25-2	North	**29**	12
	South	13	**57**
ANS MLP 740-20-2	North	**34**	7
	South	3	**67**
ANS MLP 740-24-2	North	**36**	5
	South	2	**68**
ANS MLP 740-15-2	North	**34**	7
	South	3	**67**
ANS MLP 740-8-2	North	**36**	5
	South	7	**63**

(c) Varietal classification using ANN architecture MLP 740-25-4.

Varietal	Accuracy (%)	Sensitivity (%)	Specificity (%)	Precision (%)	MCC
Chardonnay	98.2	96.2	98.8	96.2	0.950
Pinot Noir	97.3	93.3	98.8	96.6	0.931
Syrah	97.3	96.3	97.6	92.9	0.928
Sauvignon Blanc	98.2	96.4	98.8	96.4	0.952
Varietal (mean class-specific one-versus-rest metrics)[a]	97.8	95.6	98.5	95.5	0.940

(d) Confusion matrix – Varietal - ANN architecture MLP 740-25-4

Actual/Predicted	Chardonnay	Pinot Noir	Syrah	Sauvignon Blanc
Chardonnay	**25**	0	0	1
Pinot Noir	0	**28**	2	0
Syrah	0	1	**26**	0
Sauvignon Blanc	1	0	0	**27**

(e) Varietal classification using ANS architecture MLP 740-21–4.

Varietal	Accuracy (%)	Sensitivity (%)	Specificity (%)	Precision (%)	MCC
Chardonnay	100.0	100.0	100.0	100.0	1.000
Pinot Noir	99.1	100.0	98.8	96.8	0.978
Syrah	99.1	96.3	100.0	100.0	0.976
Sauvignon Blanc	100.0	100.0	100.0	100.0	1.000
Varietal (mean class-specific one-versus-rest metrics)[a]	99.5	99.1	99.7	99.2	0.988

(f) Confusion matrix – Varietal - ANS architecture MLP 740-21–4.

Actual/Predicted	Chardonnay	Pinot Noir	Syrah	Sauvignon Blanc
Chardonnay	**26**	0	0	0
Pinot Noir	0	**30**	0	0
Syrah	0	1	**26**	0
Sauvignon Blanc	0	0	0	**28**

(g) Varietal classification using ANS architecture MLP 740-23-4.

Varietal	Accuracy (%)	Sensitivity (%)	Specificity (%)	Precision (%)	MCC
Chardonnay	98.2	96.2	98.8	96.2	0.950
Pinot Noir	100.0	100.0	100.0	100.0	1.000
Syrah	99.1	96.3	100.0	100.0	0.976
Sauvignon Blanc	97.3	96.4	97.6	93.1	0.929
Varietal (mean class-specific one-versus-rest metrics)[a]	98.6	97.2	99.1	97.3	0.964

(h) Confusion matrix – Varietal - ANS architecture MLP 740-23-4.

Actual/Predicted	Chardonnay	Pinot Noir	Syrah	Sauvignon Blanc
Chardonnay	**25**	0	0	1
Pinot Noir	0	**30**	0	0
Syrah	0	0	**26**	1
Sauvignon Blanc	1	0	0	**27**

(i) Varietal classification using ANS architectures MLP 740-18-4 and MLP 740-15-4 (generated identical confusion matrices).

Variety	Accuracy (%)	Sensitivity (%)	Specificity (%)	Precision (%)	MCC

(*continued on next page*)

Table 2 (*continued*)

(i) Varietal classification using ANS architectures MLP 740-18-4 and MLP 740-15-4 (generated identical confusion matrices).

Variety	Accuracy (%)	Sensitivity (%)	Specificity (%)	Precision (%)	MCC
Chardonnay	96.4	96.2	96.5	89.3	0.903
Pinot Noir	95.5	96.7	95.1	87.9	0.891
Syrah	95.5	85.2	98.8	95.8	0.875
Sauvignon Blanc	96.4	89.3	98.8	96.2	0.903
Varietal (mean class-specific one-versus-rest metrics)[a]	96.0	91.9	97.3	92.3	0.893

(j) Confusion matrix – Varietal – ANS architectures MLP 740-18-4 and MLP 740-15-4 (generated identical confusion matrices).

Actual/Predicted	Chardonnay	Pinot Noir	Syrah	Sauvignon Blanc
Chardonnay	**25**	0	0	1
Pinot Noir	0	**29**	1	0
Syrah	0	4	**23**	0
Sauvignon Blanc	3	0	0	**25**

Note (a): MCC, Matthews correlation coefficient; sensitivity = TP/(TP + FN); specificity = TN/(TN + FP); precision = TP/(TP + FP); accuracy = (TP + TN)/(TP + TN + FP + FN).
Note (b): Rows represent actual classes and columns represent predicted classes.
Note (c): Training algorithm: BFGS 9; Error function: Entropy; Hidden-layer activation function: Tanh; Output-layer activation function: Softmax; MCC, Matthews correlation coefficient; sensitivity = TP/(TP + FN); specificity = TN/(TN + FP); precision = TP/(TP + FP); accuracy = (TP + TN)/(TP + TN + FP + FN). [a] For varietal classification, sensitivity, specificity, precision, accuracy, and MCC were calculated separately for Chardonnay, Pinot Noir, Syrah, and Sauvignon Blanc using a one-versus-rest approach. The resulting class-specific performance metrics were then averaged across classes to obtain the mean class-specific one-versus-rest metrics. The overall multiclass accuracy derived from the confusion matrix is 95.5% (106/111 correctly classified samples).
Note (d): Rows represent actual classes and columns represent predicted classes.
Note (e): Training algorithm: BFGS 39; Error function: SOS; Hidden-layer activation function: Identity; Output-layer activation function: Identity; MCC, Matthews correlation coefficient; sensitivity = TP/(TP + FN); specificity = TN/(TN + FP); precision = TP/(TP + FP); accuracy = (TP + TN)/(TP + TN + FP + FN); [a] For varietal classification, sensitivity, specificity, precision, accuracy, and MCC were calculated separately for Chardonnay, Pinot Noir, Syrah, and Sauvignon Blanc using a one-versus-rest approach. The resulting class-specific performance metrics were then averaged across classes to obtain the mean class-specific one-versus-rest metrics. The overall multiclass accuracy derived from the confusion matrix is 99.1% (110/111 correctly classified samples).
Note (f): Rows represent actual classes and columns represent predicted classes.
Note (g): Training algorithm: BFGS 33; Error function: SOS; Hidden-layer activation function: Exponential; Output-layer activation function: Logistic; MCC, Matthews correlation coefficient; sensitivity = TP/(TP + FN); specificity = TN/(TN + FP); precision = TP/(TP + FP); accuracy = (TP + TN)/(TP + TN + FP + FN); [a] For varietal classification, sensitivity, specificity, precision, accuracy, and MCC were calculated separately for Chardonnay, Pinot Noir, Syrah, and Sauvignon Blanc using a one-versus-rest approach. The resulting class-specific performance metrics were then averaged across classes to obtain the mean class-specific one-versus-rest metrics. The overall multiclass accuracy derived from the confusion matrix is 97.3% (108/111 correctly classified samples).
Note (h): Rows represent actual classes and columns represent predicted classes.
Note (i): Training algorithm: BFGS 6; Error function: Entropy; Hidden-layer activation function: Tanh; Output-layer activation function: Softmax; MCC, Matthews correlation coefficient; sensitivity = TP/(TP + FN); specificity = TN/(TN + FP); precision = TP/(TP + FP); accuracy = (TP + TN)/(TP + TN + FP + FN); [a] For varietal classification, sensitivity, specificity, precision, accuracy, and MCC were calculated separately for Chardonnay, Pinot Noir, Syrah, and Sauvignon Blanc using a one-versus-rest approach. The resulting class-specific performance metrics were then averaged across classes to obtain the mean class-specific one-versus-rest metrics. The overall multiclass accuracy derived from the confusion matrix is 91.9% (102/111 correctly classified samples).
Note (j): Rows represent actual classes and columns represent predicted classes.

(Table S1b,c). Chardonnay wines were concentrated in 2023–2024, whereas Syrah wines were more frequently represented in earlier vintages. Six of the seven 2025 wines were Sauvignon Blanc, and all 2019 and 2025 wines originated from the South Island. Thus, vintage cannot be excluded as a contributor to the observed classification patterns. Studies with a more balanced distribution of vintages across varieties and geographical origins are needed to disentangle these effects.

3.6. Classification of wines using multiclass PLS-DA

A multi-class discrimination model was developed to classify the four wine varieties using hard (deterministic) and soft (probabilistic) decision strategies (Table 4a). In multi-class PLS-DA, mean class TEFF is considered the primary indicator of model performance (Pomerantsev & Rodionova, 2021). A model with eight latent variables was selected based on training and validation performance (Fig. 3a). Hard classification achieved a mean class TEFF of 99.4%, a mean class-specific MCC of 0.988, and an overall multiclass accuracy of 99.1% (110/111), with one Pinot Noir sample misclassified as Syrah (Table S4a). Soft classification achieved a mean class efficiency of 97.9%. Under soft classification, 25 Chardonnay, 28 Pinot Noir, 27 Syrah, and 27 Sauvignon Blanc samples were accepted into their respective target classes (Table S4b). Additional acceptances occurred between Pinot Noir and Syrah, and some samples remained unassigned.

The near-perfect discrimination achieved by PLS-DA indicates that grape variety was the principal source of variation captured by the ^{1}H NMR metabolomic fingerprints. Nevertheless, terroir-related factors influence wine composition. Studies of Sauvignon Blanc vineyards in Marlborough have demonstrated spatial variability in vineyard performance associated with differences in soil properties, water availability, and climatic conditions, while recent work on spontaneous fermentations of Pinot Noir from Waipara showed that vineyard-specific microbial communities can extend terroir effects into the fermentation process (Bramley et al., 2023; Tian et al., 2025). Furthermore, metabolomic studies have shown that terroir signatures can be detected when genetic variation is controlled (Dal Santo et al., 2016). The limited overlap observed between Pinot Noir and Syrah (Table S4) may reflect residual environmental and winemaking effects superimposed on otherwise distinct varietal metabolic profiles.

3.7. Classification of wines using SB-PLSDA

SB-PLSDA was applied to discriminate wines according to geographical origin (North versus South Island). Before optimising the model, we identified potential outliers using an SB-PLSDA implementation with an outlier significance threshold of $\gamma = 0.05$. Two South Island samples were identified as outliers and removed from further analysis (Fig. 3c). Model development subsequently proceeded in the classical mode using the cleaned dataset ($n = 109$). The optimal model complexity corresponded to six latent variables (LV = 6; Fig. S3). The

Table 3
Performance of Random Forest (RF) classification for geographical origin and varietal discrimination of New Zealand wines.

(a) Classification indices

Classification task	Accuracy (%)	Sensitivity (%)	Specificity (%)	Precision (%)	MCC
Geographical origin	78.4	43.9	98.6	94.7	0.544
Varietal (mean one-versus-rest metrics)[a]	96.0	91.6	97.3	92.5	0.893
Chardonnay	93.7	76.9	98.8	95.2	0.819
Pinot Noir	98.2	96.7	98.8	96.7	0.954
Syrah	98.2	96.3	98.8	96.3	0.951
Sauvignon Blanc	93.7	96.4	92.8	81.8	0.848

(b) Confusion matrix – Geographical origin

Actual/Predicted	North	South
North	**18**	23
South	1	**69**

(c) Confusion matrix – Varietal

Actual/Predicted	Chardonnay	Pinot Noir	Syrah	Sauvignon Blanc
Chardonnay	**20**	0	0	6
Pinot Noir	0	**29**	1	0
Syrah	0	1	**26**	0
Sauvignon Blanc	1	0	0	**27**

(d) Confusion matrix – Vintage

Actual/Predicted	2019	2020	2021	2022	2023	2024	2025	Total
2019	**0**	0	0	4	0	1	0	5
2020	0	**0**	0	5	2	2	0	9
2021	0	0	**0**	9	1	3	0	13
2022	0	0	0	**16**	3	1	0	20
2023	0	0	0	5	**21**	4	0	30
2024	0	0	0	4	6	**17**	0	27
2025	0	0	0	0	5	2	**0**	7
Total	**0**	**0**	**0**	**43**	**38**	**30**	**0**	**111**

Note (a): MCC, Matthews correlation coefficient; sensitivity = TP/(TP + FN); specificity = TN/(TN + FP); precision = TP/(TP + FP); accuracy = (TP + TN)/(TP + TN + FP + FN). [a]For varietal classification, sensitivity, specificity, precision, accuracy, and MCC were calculated separately for Chardonnay, Pinot Noir, Syrah, and Sauvignon Blanc using a one-versus-rest approach and subsequently averaged across classes. The overall multiclass accuracy derived from the confusion matrix was 91.9% (102/111 correctly classified samples).
Note (b): Rows represent actual classes and columns represent predicted classes.
Note (c): Rows represent actual classes and columns represent predicted classes.
Note (d): The overall multiclass accuracy derived from the confusion matrix was 48.6% (54/111 correctly classified samples).

significance level (α) was selected from the ROC curve (Sensitivity versus 1 − Specificity; Fig. 3b), and a common α value was applied to both classes. Table 4a summarises the optimised model's classification results according to the confusion matrix (Table 4b). The model achieved a TEFF of 98.2%, with sensitivity, specificity, and precision values of 97.2%, 99.1%, and 97.6%, respectively, indicating excellent discrimination between North and South Island wines. Of the 109 samples evaluated, two Chardonnay wines, one from each island, remained unassigned, and the model incorrectly assigned one South Island Pinot Noir to the North Island class. The high specificity indicates a low false-positive rate and suggests that the SB-PLSDA model captured compositional differences related to geographical origin in the ^{1}H NMR fingerprints. Despite varietal and terroir-related variability, the model could recognise regional patterns, supporting SB-PLSDA's suitability for geographical-origin authentication of New Zealand wines.

3.8. Authentication of wines using DD-SIMCA

For the DD-SIMCA analysis, Syrah was selected as a representative example because the same modelling workflow was applied to all wine varieties. The initial model, built using all 740 spectral variables, retained two PCs and achieved a training sensitivity of 96.3% and a PCV sensitivity of 92.6%. Among the non-target classes, Pinot Noir was the nearest-of-kin class, showing the lowest selectivity (49.3%), whereas both white wine varieties were completely separated from Syrah (Fig. 4a). Application of the LOVE variable-selection procedure reduced the dataset to 442 variables (Fig. 4b) and substantially improved model performance. Table 5 presents the figures of merit for the DD-SIMCA models, with the corresponding error matrices in Table S5. Specificity was evaluated against the alternative variety specified for each target model. Although the number of PCs remained unchanged, specificity relative to Pinot Noir increased from 43.3% to 90.0%, while selectivity increased from 49.3% to 88.4%. The optimisation process maintained complete separation from Chardonnay and Sauvignon Blanc.

The same optimisation strategy was subsequently applied to all varietal models (Table 5). Variable selection increased specificity and selectivity for all four target varieties. Specificity increased from 14.8% to 81.5% for Pinot Noir, from 30.8% to 92.3% for Sauvignon Blanc, and from 75.0% to 85.7% for Chardonnay. Training and PCV sensitivities remained unchanged for Syrah, Pinot Noir, and Chardonnay. For Sauvignon Blanc, training sensitivity remained at 100.0%, whereas PCV sensitivity decreased from 96.4% to 84.6%; the optimised model also excluded sample SB29 as an outlier. Thus, LOVE reduced the variable set and improved rejection of the specified alternative varieties. These results indicate improved rejection of the specified alternative varieties, with reduced cross-validation sensitivity for Sauvignon Blanc.

DD-SIMCA is an authentication rather than a discrimination method; therefore, excessive variable reduction may be counterproductive (Masotto et al., 2026). For example, preliminary optimisation of the Sauvignon Blanc model showed that reducing the variable set to about 160 predictors further increased specificity relative to Chardonnay wines but also led to the erroneous acceptance of several Syrah samples. This indicated that improved rejection of Chardonnay came at the cost of poorer rejection of another non-target variety, highlighting the need to

Table 4
Performance of SB PLS-DA classification model for geographical origin discrimination and Multiclass PLS-DA classification models for varietal discrimination of New Zealand wines.

(a) Classification indices

Classification task	Sensitivity (%)	Specificity (%)	Precision (%)	MCC	TEFF (%)
Geographical origin	97.2	99.1	97.6	–	98.2
Varietal, Hard decision[a]	99.1	99.7	99.1	0.988	99.4
Chardonnay	100.0	100.0	100.0	–	100.0
Pinot Noir	96.7	100.0	100.0	–	98.3
Syrah	100.0	98.8	96.4	–	99.4
Sauvignon Blanc	100.0	100.0	100.0	–	100.0
Varietal, Soft decision[b]	96.5	99.4	98.2	–	97.9
Chardonnay	96.2	100.0	100.0	–	98.1
Pinot Noir	93.3	98.8	96.6	–	96.0
Syrah	100	98.8	96.4	–	99.4
Sauvignon Blanc	96.4	100.0	100.0	–	98.2

(b) Confusion matrix – Geographical origin

Actual/Predicted	North	South
North	40	0
South	1	66

Note (a): TEFF = mean class efficiency; [a] Overall multiclass accuracy calculated from the confusion matrix was 99.1% (110/111 correctly classified samples); [b] Under soft classification, 107 of 111 samples (96.4%) were accepted into their true class; this percentage includes samples that may also have been accepted into another class.
Note (b): 2 samples were not assigned to any class.

assess all available alternative classes during optimisation. Consequently, we selected the final optimised models to balance sensitivity, specificity, and selectivity while preserving DD-SIMCA's authentication capability. The optimised models retained different subsets of spectral variables (Fig. 4c), indicating that different spectral features contributed to modelling each target variety, reflecting its distinct metabolomic fingerprint. Further improvements in authentication performance may be achieved by increasing sample size and integrating complementary analytical methods, as DD-SIMCA is well suited to high-level data fusion strategies (dos Santos et al., 2026).

4. Conclusions

Untargeted ^{1}H NMR metabolomic fingerprinting, combined with chemometric and machine-learning approaches, supported discrimination of New Zealand wines by grape variety and island of origin. ANS varietal model correctly classified 110 of 111 wines. Vintage classification achieved overall accuracies below 50% for SVM and RF. However, vintage was unevenly distributed across varieties and geographical origins, and its contribution to the observed classification patterns cannot be excluded. SVM and RF achieved higher overall accuracy for varietal than geographical-origin classification. Hard-decision PLS-DA achieved high varietal discrimination efficiency, and SB-PLSDA showed remarkable geographical-origin discrimination after outlier exclusion. LOVE-based variable selection improved DD-SIMCA specificity against closely related wine varieties. These findings demonstrate the potential of ^{1}H NMR fingerprints for wine discrimination and authentication within the studied dataset. Larger, independently collected validation sets (e.g., more samples from each variety, vintages, and geographical origins) are needed to establish generalisability, while complementary targeted metabolomics analyses could improve metabolite annotation and clarify the compositional differences associated with variety and geographical origin.

Declaration of generative AI and AI-assisted technologies in the manuscript preparation process

During the preparation of this work, the authors used ChatGPT

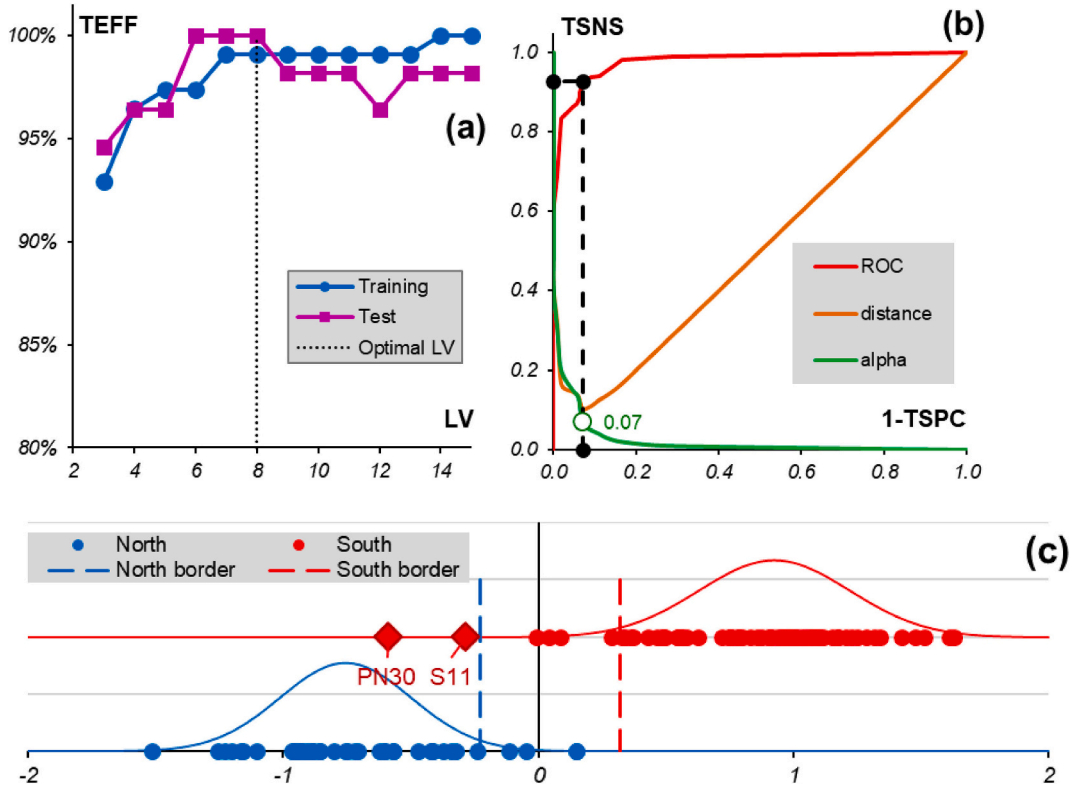


Fig. 3. PLS-DA modelling. (a) Selection of LV in hard PLS-DA; (b) Selection of α in SB PLS-DA; (c) Acceptance plot in SB PLS-DA with two outliers.

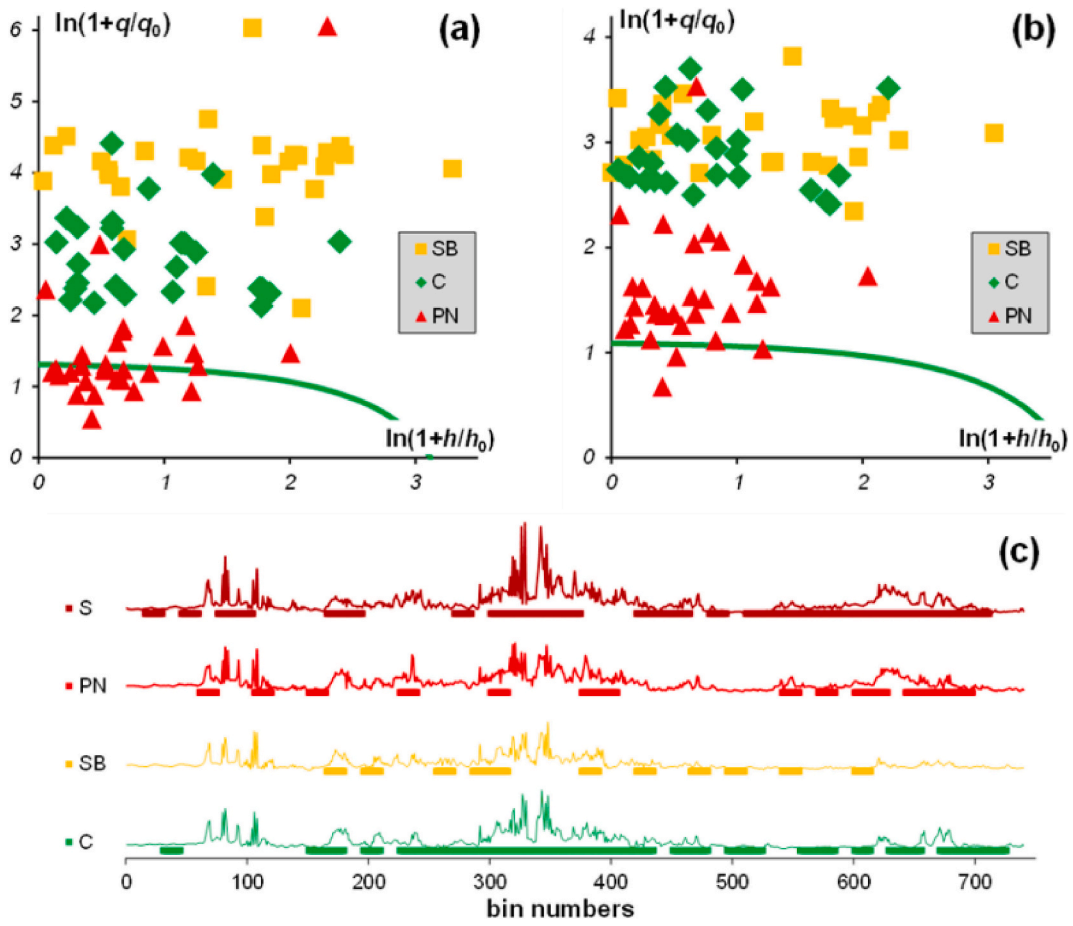


Fig. 4. (a) DD-SIMCA modelling. Prediction of classes that are alternatives for the Syrah variety (target) in the case of the full dataset and the optimised dataset (b); (c) Variable selection: dots indicate the selected variables, and the corresponding curves represent scaled NMR spectra.

Table 5
Figures of merit for DD-SIMCA one-class authentication models developed for Syrah, Pinot Noir, Chardonnay, and Sauvignon Blanc wines.

Target dataset	Number of variables	PCs	Sensitivity training (%)	Sensitivity PCV (%)	Specificity* (%)	Selectivity** (%)
Syrah Full**	740	2	96.3	92.6	43.3	49.3
Syrah Optimised	442	2	96.3	92.6	90.0	88.4
Pinot Noir Full**	740	4	100.0	83.3	14.8	12.9
Pinot Noir Optimised	219	4	100.0	83.3	81.5	83.2
Chardonnay Full**	740	2	100.0	96.2	75.0	69.8
Chardonnay Optimised	458	2	100.0	96.2	85.7	81.9
Sauvignon Blanc Full**	740	3	100.0	96.4	30.8	32.8
Sauvignon Blanc Optimised***	489	3	100.0	84.6	92.3	83.6

Note: *All optimised models demonstrate 100% specificity regarding the wine types (e.g., red vs white wines). ** Specificity and selectivity are calculated for the Syrah model relative to Pinot Noir, for the Pinot Noir model relative to Syrah samples, for the Chardonnay model relative to Sauvignon Blanc, and for Sauvignon Blanc relative to Chardonnay. *** The optimised model is built without one outlier, SB29.

(OpenAI) to recheck classification performance metrics previously calculated manually in Microsoft Excel from confusion matrices and to improve the manuscript's clarity and conciseness. After using this tool, the authors reviewed and edited the content as needed and take full responsibility for the content of the published article.

CRediT authorship contribution statement

Bruno Toribio de Lima Xavier: Writing – original draft, Investigation, Formal analysis, Data curation. **Rushan Dissanayake Mudiyanselage:** Writing – original draft, Software, Methodology, Formal analysis. **Adrian Owens:** Writing – original draft, Software, Methodology, Formal analysis, Data curation. **Oxana Ye Rodionova:** Writing – original draft, Methodology, Formal analysis, Data curation. **Alexey L. Pomerantsev:** Writing – original draft, Software, Formal analysis, Data curation. **Daniel Granato:** Writing – original draft, Validation, Supervision, Software, Resources, Project administration, Funding acquisition, Formal analysis, Data curation, Conceptualization.

Ethical statement

This research did not require research ethics committee approval.

Declaration of competing interest

The authors declare that they have no known competing financial interests or personal relationships that could have appeared to influence the work reported in this paper.

Acknowledgements

The authors thank the AUT Faculty of Health and Environmental Sciences for funding this research (REFI-21593) and the School of Science for initial funds granted to D. Granato. The authors thank Flaticon, BioRender App, and Illustrae for the icons used in the graphical abstract.

Appendix A. Supplementary data

Supplementary data to this article can be found online at https://doi.org/10.1016/j.foodres.2026.121157.

Data availability

Data will be made available on request.

References

Ali, K., Maltese, F., Toepfer, R., Choi, Y. H., & Verpoorte, R. (2011). Metabolic characterization of Palatinate German white wines according to sensory attributes, varieties, and vintages using NMR spectroscopy and multivariate data analyses. *Journal of Biomolecular NMR, 49*(3–4), 255–266. https://doi.org/10.1007/s10858-011-9487-3

An, J., & Liu, C. (2026). Developing cost-effective soft sensors to predict wine extrinsic attributes using selected chemical parameters. *Food and Humanity, 7*, Article 101398. https://doi.org/10.1016/j.foohum.2026.101398

Babamoradi, H., van den Berg, F., & Rinnan, Å. (2013). Bootstrap based confidence limits in principal component analysis — A case study. *Chemometrics and Intelligent Laboratory Systems, 120*, 97–105. https://doi.org/10.1016/j.chemolab.2012.10.007

Bambina, P., Spinella, A., Lo Papa, G., Chillura Martino, D. F., Lo Meo, P., Cinquanta, L., & Conte, P. (2024). 1H-NMR spectroscopy coupled with chemometrics to classify wines according to different grape varieties and different terroirs. *Agriculture, 14*(5), Article 749. https://doi.org/10.3390/agriculture14050749

Barátossy, G., Berinkeiné Donkó, M., Csikorné Vásárhelyi, H., Héberger, K., & Rácz, A. (2021). Comprehensive classification and regression modeling of wine samples using 1H NMR spectra. *Foods, 10*(1), Article 64. https://doi.org/10.3390/foods10010064

Bobáľ, B., Ješkovský, M., Kaizer, J., Kontuľ, I., Bujdoš, M., & Povinec, P. P. (2025). Elemental analysis of selected wines by particle induced X-ray emission (PIXE) for determination of geographical origin. *Applied Radiation and Isotopes, 226*, Article 112234. https://doi.org/10.1016/j.apradiso.2025.112234

Bramley, R. G. V., Ouzman, J., Sturman, A. P., Grealish, G. J., Ratcliff, C. E. M., & Trought, M. C. T. (2023). Underpinning terroir with data: Integrating vineyard performance metrics with soil and climate data to better understand within-region variation in Marlborough, New Zealand. *Australian Journal of Grape and Wine Research, 2023*, 1–23. https://doi.org/10.1155/2023/8811402

Chicco, D., & Jurman, G. (2020). The advantages of the Matthews correlation coefficient (MCC) over F1 score and accuracy in binary classification evaluation. *BMC Genomics, 21*(1), 6. https://doi.org/10.1186/s12864-019-6413-7

Cosme, F., Milheiro, J., Pires, J., Guerra-Gomes, F. I., Filipe-Ribeiro, L., & Nunes, F. M. (2021). Authentication of Douro DO monovarietal red wines based on anthocyanin profile: Comparison of partial least squares – Discriminant analysis, decision trees and artificial neural networks. *Food Control, 125*, Article 107979. https://doi.org/10.1016/j.foodcont.2021.107979

Crook, A. A., Zamora-Olivares, D., Bhinderwala, F., Woods, J., Winkler, M., Rivera, S., Shannon, C. E., Wagner, H. R., Zhuang, D. L., Lynch, J. E., Berryhill, N. R., Runnebaum, R. C., Anslyn, E. V., & Powers, R. (2021). Combination of two analytical techniques improves wine classification by vineyard, region, and vintage. *Food Chemistry, 354*, Article 129531. https://doi.org/10.1016/j.foodchem.2021.129531

Dal Santo, S., Commisso, M., D'Incà, E., Anesi, A., Stocchero, M., Zenoni, S., Ceoldo, S., Tornielli, G. B., Pezzotti, M., & Guzzo, F. (2016). The terroir concept interpreted through grape berry metabolomics and transcriptomics. *Journal of Visualized Experiments, 116*. https://doi.org/10.3791/54410

Delić, K., Milinčić, D. D., Pešić, M. B., Steva Lević, S., Nedović, V. A., Gancel, A.-L., Jourdes, M., & Teissedre, P.-L. (2024). Grape, wine and pomace anthocyanins: Winemaking biochemical transformations, application and potential benefits. *OENO one, 58*(4). https://doi.org/10.20870/oeno-one.2024.58.4.8039

dos Santos, L. B., Augusti, R., Nascentes, C. C., Sena, M. M., & Almeida, M. R. (2026). One-class modeling for the authentication of a geographically certified Brazilian coffee based on atomic-molecular data fusion. *Food Chemistry, 498*, Article 147158. https://doi.org/10.1016/j.foodchem.2025.147158

Du, Y., Bai, G., Zhang, X., & Liu, M. (2007). Classification of wines based on combination of ^{1}H NMR spectroscopy and principal component analysis. *Chinese Journal of Chemistry, 25*(7), 930–936. https://doi.org/10.1002/cjoc.200790181

Ehlers, M., Horn, B., Raeke, J., Fauhl-Hassek, C., Hermann, A., Brockmeyer, J., & Riedl, J. (2022). Towards harmonization of non-targeted 1H NMR spectroscopy-based wine authentication: Instrument comparison. *Food Control, 132*, Article 108508. https://doi.org/10.1016/j.foodcont.2021.108508

García-Aguilera, M. E., Delgado-Altamirano, R., Villalón, N., Ruiz-Terán, F., García-Garnica, M. M., Ocaña-Ríos, I., Rodríguez de San Miguel, E., & Esturau-Escofet, N. (2023). Study of the stability of wine samples for 1H-NMR metabolomic profile analysis through chemometrics methods. *Molecules, 28*(16), Article 5962. https://doi.org/10.3390/molecules28165962

Gorodkin, J. (2004). Comparing two K-category assignments by a K-category correlation coefficient. *Computational Biology and Chemistry, 28*(5–6), 367–374. https://doi.org/10.1016/j.compbiolchem.2004.09.006

Gougeon, L., da Costa, G., Guyon, F., & Richard, T. (2019). 1H NMR metabolomics applied to Bordeaux red wines. *Food Chemistry, 301*, Article 125257. https://doi.org/10.1016/j.foodchem.2019.125257

Gougeon, R. D., Lucio, M., Frommberger, M., Peyron, D., Chassagne, D., Alexandre, H., Feuillat, F., Voilley, A., Cayot, P., Gebefügi, I., Hertkorn, N., & Schmitt-Kopplin, P. (2009). The chemodiversity of wines can reveal a metabologeography expression of cooperage oak wood. *Proceedings of the National Academy of Sciences, 106*(23), 9174–9179. https://doi.org/10.1073/pnas.0901100106

Green, J. A., Parr, W. V., Breitmeyer, J., Valentin, D., & Sherlock, R. (2011). Sensory and chemical characterisation of sauvignon blanc wine: Influence of source of origin. *Food Research International, 44*(9), 2788–2797. https://doi.org/10.1016/j.foodres.2011.06.005

Han, S., Yang, J., Choi, K., Kim, J., Adhikari, K., & Lee, J. (2022). Chemical analysis of commercial white wines and its relationship with consumer acceptability. *Foods, 11*(4), Article 603. https://doi.org/10.3390/foods11040603

Hategan, A. R., David, M., Pirnau, A., Cozar, B., Cinta-Pinzaru, S., Guyon, F., & Magdas, D. A. (2024). Fusing 1H NMR and Raman experimental data for the improvement of wine recognition models. *Food Chemistry, 458*, Article 140245. https://doi.org/10.1016/j.foodchem.2024.140245

Hiniesta-Valero, J., Guerra-Castellano, A., Fernández-Veloso, A., De la Rosa, M. A., & Díaz-Moreno, I. (2025). A machine learning-based nuclear magnetic resonance profiling model to authenticate 'Jerez-Xérès-Sherry' wines. *Spectrochimica Acta Part A: Molecular and Biomolecular Spectroscopy, 337*, Article 126102. https://doi.org/10.1016/j.saa.2025.126102

International Organisation of Vine and Wine Intergovernmental Organisation. (2025). STATE OF THE WORLD VINE AND WINE SECTOR IN 2024. , April https://www.oiv.int/sites/default/files/2025-04/OIV-State_of_the_World_Vine-and-Wine-Sector-in-2024.pdf.

Jagatić Korenika, A.-M., Jeromel, A., Tomaz, I., Jednačak, T., Rončević, S., Nemet, I., Primožič, I., Hrenar, T., & Novak, P. (2024). Deep reinforcement learning classification of sparkling wines based on ICP-MS and DOSY NMR spectra. *Food Chemistry: X, 21*, Article 101162. https://doi.org/10.1016/j.fochx.2024.101162

Karapetsas, N., Alexandridis, T. K., Bilas, G., Theocharis, S., & Koundouras, S. (2023). Delineating natural terroir units in wine regions using geoinformatics. *Agriculture, 13*(3), Article 629. https://doi.org/10.3390/agriculture13030629

Keller, S. T., Harner, A. D., Centinari, M., Elias, R. J., & Hopfer, H. (2021). Influence of region on sensory and chemical profiles of Pennsylvania Grüner Veltliner wines. *Foods, 10*(4), Article 825. https://doi.org/10.3390/foods10040825

Khakimov, B., Bakhytkyzy, I., Fauhl-Hassek, C., & Engelsen, S. B. (2022). Non-volatile molecular composition and discrimination of single grape white wines of chardonnay, Riesling, sauvignon Blanc and Silvaner using untargeted GC-MS analysis. *Food Chemistry, 369*, Article 130878. https://doi.org/10.1016/j.foodchem.2021.130878

Kucheryavskiy, S., Rodionova, O., & Pomerantsev, A. (2024). A comprehensive tutorial on data-driven SIMCA: Theory and implementation in web. *Journal of Chemometrics, 38*(7). https://doi.org/10.1002/cem.3556

Le Mao, I., Da Costa, G., Bautista, C., de Revel, G., & Richard, T. (2023). Application of 1H NMR metabolomics to French sparkling wines. *Food Control, 145*, Article 109423. https://doi.org/10.1016/j.foodcont.2022.109423

Le Mao, I., Da Costa, G., Leleu, G., & Richard, T. (2024). Monitoring red wine maturation in oak barrels using 1H NMR-based metabolomics. *OENO one, 58*(2). https://doi.org/10.20870/oeno-one.2024.58.2.7465

Le Mao, I., Da Costa, G., & Richard, T. (2023). 1H-NMR metabolomics for wine screening and analysis. *OENO one, 57*(1), 15–31. https://doi.org/10.20870/oeno-one.2023.57.1.7134

Le Mao, I., Martin-Pernier, J., Bautista, C., Lacampagne, S., Richard, T., & Da Costa, G. (2021). 1H-NMR metabolomics as a tool for winemaking monitoring. *Molecules, 26*(22), Article 6771. https://doi.org/10.3390/molecules26226771

Lee, B. L., Rout, M., Dong, Y., Lipfert, M., Berjanskii, M., Shahin, F., Bhattacharyya, D., Selim, A., Mandal, R., & Wishart, D. S. (2024). Automatic chemical profiling of wine by proton nuclear magnetic resonance spectroscopy. *ACS Food Science & Technology, 4*(8), 1937–1949. https://doi.org/10.1021/acsfoodscitech.4c00298

Leleu, G., Butelle, R., Jacob, D., Kurkiewicz, L.-A., Boulet, J.-C., Deborde, C., Dubernet, M., Gaillard, L., Galvan, A., Gaudin, K., Gossé, A., Herderich, M., Moing, A., Rosset, S., Watson, F., Da Costa, G., & Richard, T. (2026). 1H-NMR analysis of wine metabolites: Method development and validation. *Molecules, 31*(1), Article 65. https://doi.org/10.3390/molecules31010065

López-Rituerto, E., Cabredo, S., López, M., Avenoza, A., Busto, J. H., & Peregrina, J. M. (2009). A thorough study on the use of quantitative ^{1}H NMR in Rioja red wine fermentation processes. *Journal of Agricultural and Food Chemistry, 57*(6), 2112–2118. https://doi.org/10.1021/jf803245r

Mascellani, A., Hoca, G., Babisz, M., Krska, P., Kloucek, P., & Havlik, J. (2021). 1H NMR chemometric models for classification of Czech wine type and variety. *Food Chemistry, 339*, Article 127852. https://doi.org/10.1016/j.foodchem.2020.127852

Masotto, E., Horacek, M., Zitek, A., Hann, S., & Jandric, Z. (2026). Mass spectrometry-based authentication of PDO "Wachauer Marille" using DD-SIMCA one-class classification. *Food Chemistry, 527*, Article 150915. https://doi.org/10.1016/j.foodchem.2026.150915

Ministry for Primary Industries. (2003). Wine Act 2003. https://www.legislation.govt.nz/act/public/2003/114/en/latest/#DLM222447.

Muhl, J. R., Pilkington, L. I., Fedrizzi, B., & Deed, R. C. (2025). Investigating the factors driving concentrations of volatile thiols and their precursors in white wines: The impact of Botrytis cinerea and grape variety. *Food Chemistry, 479*, Article 143551. https://doi.org/10.1016/j.foodchem.2025.143551

New Zealand Wine. (2025). Why New Zealand remains the benchmark for modern sauvignon Blanc. https://www.nzwine.com/en/media/story/benchmark/.

New Zealand Winegrowers. (2026). New Zealand wine KPIs: July 2026. https://www.nzwine.com/en/media/statistics-reports/nz-wine-kpis/.

Phan, Q., & Tomasino, E. (2021). Untargeted lipidomic approach in studying pinot noir wine lipids and predicting wine origin. *Food Chemistry, 355*, Article 129409. https://doi.org/10.1016/j.foodchem.2021.129409

Pomerantsev, A. L., Kucheryavskiy, S., & Rodionova, O. Y. (2025). Variable selection for one class classifiers. Introduction of LOVE. *Analytica Chimica Acta, 1368*, Article 344302. https://doi.org/10.1016/j.aca.2025.344302

Pomerantsev, A. L., & Rodionova, O. Y. (2018). Multiclass partial least squares discriminant analysis: Taking the right way—A critical tutorial. *Journal of Chemometrics, 32*(8). https://doi.org/10.1002/cem.3030

Pomerantsev, A. L., & Rodionova, O. Y. (2021). New trends in qualitative analysis: Performance, optimization, and validation of multi-class and soft models. *TrAC Trends in Analytical Chemistry, 143*, Article 116372. https://doi.org/10.1016/j.trac.2021.116372

Pomerantsev, A. L., & Rodionova, O. Y. (2026). Mislabeling (label noise) – An often overlooked issue in chemometrics. *Analytica Chimica Acta, 1424*, Article 346227. https://doi.org/10.1016/j.aca.2026.346227

Priyadharshini, D., Muthuvel, I., Saraswathy, S., Balakrishnan, M., Raveendran, M., & Ramalakshmi, A. (2025). Terroir unveiled: The interplay of environment, microbes, and craft in wine making. *European Food Research and Technology, 251*(7), 1489–1498. https://doi.org/10.1007/s00217-025-04750-w

Ranaweera, R. K. R., Gilmore, A. M., Capone, D. L., Bastian, S. E. P., & Jeffery, D. W. (2021). Authentication of the geographical origin of Australian cabernet sauvignon wines using spectrofluorometric and multi-element analyses with multivariate statistical modelling. *Food Chemistry, 335*, Article 127592. https://doi.org/10.1016/j.foodchem.2020.127592

Roullier-Gall, C., Witting, M., Moritz, F., Gil, R. B., Goffette, D., Valade, M., Schmitt-Kopplin, P., & Gougeon, R. D. (2016). Natural oxygenation of champagne wine during ageing on lees: A metabolomics picture of hormesis. *Food Chemistry, 203*, 207–215. https://doi.org/10.1016/j.foodchem.2016.02.043

Sokolova, M., & Lapalme, G. (2009). A systematic analysis of performance measures for classification tasks. *Information Processing & Management, 45*(4), 427–437. https://doi.org/10.1016/j.ipm.2009.03.002

Son, H.-S., Hwang, G.-S., Ahn, H.-J., Park, W.-M., Lee, C.-H., & Hong, Y.-S. (2009). Characterization of wines from grape varieties through multivariate statistical analysis of 1H NMR spectroscopic data. *Food Research International, 42*(10), 1483–1491. https://doi.org/10.1016/j.foodres.2009.08.006

Su, Y., Yang, Y., Kilmartin, P. A., & Araujo, L. D. (2025). Inter-regional characterization of New Zealand pinot noir wines: Assessing geographical origin through mid-FTIR and phenolic profile analysis. *Food Research International, 212*, Article 116485. https://doi.org/10.1016/j.foodres.2025.116485

Tian, B., Dhami, M., Moukarzel, R., Zhang, J., On, S., Wimalasiri, P., Araujo, L. D., & Maxwell, D. (2025). Extending the influence of terroir through the spontaneous fermentation of pinot noir in the vineyard: A case study of Greystone vineyard fermentation. *Journal of Agricultural and Food Chemistry, 73*(14), 8531–8542. https://doi.org/10.1021/acs.jafc.4c11268

Tzachristas, A., Dasenaki, M. E., Aalizadeh, R., Thomaidis, N. S., & Proestos, C. (2021). Development of a wine metabolomics approach for the authenticity assessment of selected Greek red wines. *Molecules, 26*(10), Article 2837. https://doi.org/10.3390/molecules26102837

Urtubia, A., León, R., & Vargas, M. (2021). Identification of chemical markers to detect abnormal wine fermentation using support vector machines. *Computers & Chemical Engineering, 145*, Article 107158. https://doi.org/10.1016/j.compchemeng.2020.107158

Vacchina, V., Pieracci, Y., Di Stasi, M., Mercanti, N., Cazorla Ares, C., Rodriguez, P., Lahüt, C., Séby, F., & Donard, O. F. X. (2026). Analytical strategies combining multi-elemental isotopic dilution with external calibration for rapid and precise inorganic wine profiling by ICP-QQQ-MS: High geographic discrimination for improved wine management and traceability. *Food Chemistry, 515*, Article 149221. https://doi.org/10.1016/j.foodchem.2026.149221

Viskić, M., Bandić, L. M., Korenika, A.-M. J., & Jeromel, A. (2021). NMR in the service of wine differentiation. *Foods, 10*(1), Article 120. https://doi.org/10.3390/foods10010120

Vitale, R., & Saccenti, E. (2018). Comparison of dimensionality assessment methods in principal component analysis based on permutation tests. *Chemometrics and Intelligent Laboratory Systems, 181*, 79–94. https://doi.org/10.1016/j.chemolab.2018.08.008